AFWAL-TR-81-3096

EVALUATION OF SEVERAL BONDING PARAMETERS ON THE RANDOM BENDING FATIGUE LIFE OF ADHESIVELY BONDED ALUMINUM JOINTS

STRUCTURAL INTEGRITY BRANCH
STRUCTURES AND DYNAMICS DIVISION
FLIGHT DYNAMICS LABORATORY

COMPOSITES, ADHESIVES AND FIBROUS MATERIALS BRANCH
NONMETALLIC MATERIALS DIVISION
MATERIALS LABORATORY

AUGUST 1981

TECHNICAL REPORT AFWAL-TR-81-3096
Final Report for Period June 1978 — November 1980

FLIGHT DYNAMICS LABORATORY
AIR FORCE WRIGHT AERONAUTICAL LABORATORIES
AIR FORCE SYSTEMS COMMAND
WRIGHT- PATTERSON AIR FORCE BASE, OHIO 45433

NOTICE

When Government drawings, specifications, or other data are used for any purpose other than in connection with a definitely related Government procurement operation, the United States Government thereby incurs no responsibility nor any obligation whatsoever; and the fact that the government may have formulated, furnished, or in any way supplied the said drawings, specifications, or other data, is not to be regarded by implication or otherwise as in any manner licensing the holder or any other person or corporation, or conveying any rights or permission to manufacture use, or sell any patented invention that may in any way be related thereto.

This report has been reviewed by the Office of Public Affairs (ASD/PA) and is releasable to the National Technical Information Service (NTIS). At NTIS, it will be available to the general public, including foreign nations.

This technical report has been reviewed and is approved for publication.

Howard F. Wolfe
HOWARD F. WOLFE, Technical Manager
Acoustics and Sonic Fatigue Group

Herbert S. Schwartz
HERBERT S. SCHWARTZ
Materials Research Engineer

Carl L. Rupert
CARL L. RUPERT, Aerospace Engineer
Acoustics and Sonic Fatigue Group

Davey L. Smith
DAVEY L. SMITH
Chief, Structural Integrity Branch

Theodore J. Reinhart
THEODORE J. REINHART
Chief, Composites, Adhesives and
Fibrous Materials Branch

FOR THE COMMANDER

Ralph L. Kuster, Jr.
RALPH L. KUSTER, Jr., Colonel, USAF
Chief, Structures and Dynamics Division
Flight Dynamics Laboratory

F. D. Cherry
FRANKLIN D. CHERRY
Chief, Nonmetallic Materials Division
Materials Laboratory

"If your address has changed, if you wish to be removed from our mailing list, or if the addressee is no longer employed by your organization please notify AFWAL/FIBED *W-PAFB, OH 45433 to help us maintain a current mailing list".*

Copies of this report should not be returned unless return is required by security considerations, contractual obligations, or notice on a specific document.

AIR FORCE/56780/27 October 1981 — 630

UNCLASSIFIED

SECURITY CLASSIFICATION OF THIS PAGE *(When Data Entered)*

REPORT DOCUMENTATION PAGE		READ INSTRUCTIONS BEFORE COMPLETING FORM
1. REPORT NUMBER AFWAL-TR-81-3096	2. GOVT ACCESSION NO.	3. RECIPIENT'S CATALOG NUMBER
4. TITLE *(and Subtitle)* EVALUATION OF SEVERAL BONDING PARAMETERS ON THE RANDOM BENDING FATIGUE LIFE OF ADHESIVELY BONDED ALUMINUM JOINTS		5. TYPE OF REPORT & PERIOD COVERED Final June 78 - Nov 80 6. PERFORMING ORG. REPORT NUMBER
7. AUTHOR(s) H. F. Wolfe C. L. Rupert H. S. Schwartz		8. CONTRACT OR GRANT NUMBER(s)
9. PERFORMING ORGANIZATION NAME AND ADDRESS Air Force Wright Aeronautical Laboratories (FIBED) Wright-Patterson AFB, Ohio, 45433		10. PROGRAM ELEMENT, PROJECT, TASK AREA & WORK UNIT NUMBERS 24010146
11. CONTROLLING OFFICE NAME AND ADDRESS Air Force Wright Aeronautical Laboratories (FIBED) Wright-Patterson AFB, Ohio, 45433		12. REPORT DATE August 1981 13. NUMBER OF PAGES 57
14. MONITORING AGENCY NAME & ADDRESS *(if different from Controlling Office)*		15. SECURITY CLASS. *(of this report)* Unclassified 15a. DECLASSIFICATION/DOWNGRADING SCHEDULE

16. DISTRIBUTION STATEMENT *(of this Report)*

Approved for Public Release; Distribution Unlimited

17. DISTRIBUTION STATEMENT *(of the abstract entered in Block 20, if different from Report)*

18. SUPPLEMENTARY NOTES

19. KEY WORDS *(Continue on reverse side if necessary and identify by block number)*

Sonic Fatigue, Acoustic Fatigue, Fatigue Strength of Bonded Aluminum Joints

20. ABSTRACT *(Continue on reverse side if necessary and identify by block number)*

Eighteen adhesively bonded aluminum coupons were tested on a vibration shaker at room temperature to determine the effects of varying the adhesive type/thickness, primer and adherend surface preparation on their random bending fatigue life. Most of the fatigue failures occurred within 10^6 to 10^7 cycles, all at 900 microstrain. While neither the primer thickness nor the surface treatment seemed to influence the overall results, the coupons with thicker adhesive had a noticable shorter fatigue life. Fractographic analyses of the failed

DD FORM 1 JAN 73 1473 EDITION OF 1 NOV 65 IS OBSOLETE

UNCLASSIFIED

SECURITY CLASSIFICATION OF THIS PAGE *(When Data Entered)*

adhesive surfaces showed the locus of fracture for all coupons was predominantly within the adhesive. The nitrile phenolic adhesive demonstrated a better fatigue resistance than the nitrile epoxy.

FOREWORD

This work was performed as a joint effort by the Flight Dynamics Laboratory and the Materials Laboratory of the Air Force Wright Aeronautical Laboratories, Wright-Patterson Air Force Base, Ohio. The work was conducted under Work Unit 24010146, "Sonic Fatigue Test of Advanced Materials."

The manuscript was released for publication by the authors in May 1981.

TABLE OF CONTENTS

LIST OF ILLUSTRATIONS

LIST OF ILLUSTRATIONS

LIST OF TABLES

SECTION I

INTRODUCTION AND BACKGROUND

The development of durable high strength adhesives leads to increased interest in applying bonding technology to aircraft structures. The benefits of bonding structures include increased fatigue life, improved failsafe capabilities and lowered manufacturing costs. Cost studies determined that the high costs in airframe construction are due to the large number of holes and fasteners required and the time required to assemble the parts. Adhesive joining of components can save both weight and cost by reducing the number of parts required.

Sonic fatigue failures in riveted structures resulted in unacceptable maintenance and inspection burdens associated with aircraft operations. In some cases, sonic fatigue failures resulted in a major redesign effort of the structural components. The phenomenon manifests itself as fatigue cracks in skin panels, ribs, spars, stringers and longerons. These fatigue failures result from the vibratory response of the structure to high intensity noise. Noise sources include jet propulsion noise, turbulent boundary layer noise, separated flow noise, flow impingement and scrubbing flow effects. These noise sources produce a fluctuating pressure field which excites various structural modes. The resonant response of these structures to fluctuating pressure fields produces a very rapid stress reversal which will result in fatigue failure if the stress reversals are of sufficient magnitude.

Fatigue data are needed for adhesively bonded structural designs to determine the life of the joint as a function of the magnitude of the stress levels. These data form the basis for the design criteria needed to determine the sonic fatigue life of adhesively bonded structures and to prevent premature structural failure from acoustic excitation.

The Materials Laboratory (ML) and the Flight Dynamics Laboratory (FDL) of the Air Force Wright Aeronautical Laboratories (AFWAL) conducted several research and development programs investigating adhesives including their manufacturing processes, structural properties, and application to adhesively bonded aluminum structures. This paper describes a test and evaluation program to determine the effects of adhesive thickness, primer thickness and the type of oxide layer on the random bending fatigue life sensitivity of an adhesively bonded metallic joint.

SECTION II

TESTING APPROACH

Since many of the factors that affect sonic fatigue life of a structure are not analytically predictable, design criteria are developed using an empirical approach. A broad base of general design information in the form of nomographs, using both analytical and empirical approaches, was developed and summarized in "Sonic Fatigue Design Guide for Military Aircraft."[1] The procedure for predicting the sonic fatigue life of a structure is to determine the acoustic loads, the fundamental mode frequency, the maximum root mean square (RMS) stress at a reference position, and the number of cycles (N) to failure from an appropriate S-N curve.

S-N curves were developed for various riveted configurations by using simple panels in an acoustic test facility. The panel construction was identical to the aircraft structural component of interest and subjected to an acoustic load under laboratory conditions which very closely simulate the acoustic field produced in-service by the aircraft. A simple and less costly approach is to test a cantilever beam coupon section of the panel including the joint on a vibration shaker. The panel and coupon data are then correlated to determine their relationship. Although significant differences can exist between panel tests and shaker beam tests, various investigations show that, in most cases, these differences are negligible. While the stresses in a panel are bi-axial, in a simple joint the stress is unidirectional. In an acoustic fatigue test a broadband excitation is applied, whereas, the simple joint specimens are usually excited by a narrow frequency band. References 2 and 3 show that, when stiffened aircraft panels are excited by acoustic noise, one mode frequently predominates the response spectrum. Therefore, the problem can be treated as a single degree-of-freedom dynamics system. Most

sonic fatigue design methods are based on this proposition. Various investigations of multimodal response versus single mode response have been made.[4] Very little differences are found in the life of the structures excited with either wideband or narrowband input. It was concluded that random fatigue data obtained with a narrowband excitation of a single mode were slightly conservative when applied to structural response in a multimodal or broadband fashion.

The narrowband random amplitude vibration testing of simple structural joint samples for the purpose of generating fatigue design data for aircraft structures is an accepted practice. These data are considered as supplemental data to acoustic fatigue tests as they are used to define a fatigue curve for a particular joint.

SECTION III

PREVIOUS INVESTIGATIONS

Previous investigations of weldbonded aluminum structures and various adhesively bonded aluminum structures are summarized in Reference 5. The structures tested consisted of both panels and cantilever beam coupons. Several types of fatigue failures were obtained from these tests; however, one consistent predictable failure mode must be produced in order to develop a S-N curve from which the fatigue life can be predicted. The failures in the adhesive bond system were classified as either cohesive or adhesive failures by visual inspection without magnification. A cohesive bond failure is defined as one in which part of the adhesive remains on both adherends after failure. An adhesive bond failure is defined as a complete separation of the adhesive from one adherend while remaining on the other adherend. Generally, adhesive failures are considered undesirable. A much lower fatigue strength resulted from adhesive failure mode than the cohesive failure mode. Also, the life of the adhesive failure mode is generally more unpredictable. Many of the failures could not be clearly identified as either "cohesive" or "adhesive" failures. Portions of the bond areas in some of the test structures exhibited both.

Most of the cantilever beam coupons were tested only until the fatigue crack propagated part way through the bond area. The bond area was examined after static loading the adhesive joint until it completely separated. It could be seen that initial cracking in the adhesive under dynamic loading was different than that produced by the static pull. The static pull generally was characterized by a separation midway through the thickness of the adhesive film; whereas, under dynamic load the adhesive separated closer to the

surface of the adherend. The difference in these two mechanisms observed under dynamic loading and static loading are shown in Figure 1. To determine the sonic fatigue life of a bonded structure, the behavior of the adhesive under dynamic loading must be defined and predictable.

Another area of concern was quality control, since different results often were obtained when the test structures were fabricated by different manufacturers using the same standards. Therefore, an investigation was conducted of the adhesive/primer systems used in the Primary Adhesively Bonded Structural Technology (PABST) program sponsored by the Flight Dynamics Laboratory. These included adhesive/primer systems with phosphoric acid anodized aluminum adherends: FM73/BR127, M1133/BR127, AF55/XA3950, and EA9628/EA9202.

The FM73/BR127, with the surface preparation according to Boeing specification BAC5555, was then selected for more detailed investigation. Consequently, a follow-on program was conducted to evaluate 18 cantilever beam coupons and ten acoustic panels using this bond system. The fractured adhesive surfaces were evaluated using a scanning electron microscope (SEM) which indicated that the coupon failures were cohesive and essentially in the primer near the adhesive/primer interface. An evaluation of a panel fabricated at the same time indicated that the failure was cohesive within the primer on the skin close to the upper surface of the phosphoric acid anodize layer. In both cases, behavior of the primer became the principal concern.

The fatigue lives of the beam coupons were not noticeably different from those of the previous tests where detailed inspections of the fracture surfaces were not performed. The questions remaining unanswered from the previous investigations are how the adhesive thickness, primer thickness and the type of oxide layer affect the fatigue life of the joint.

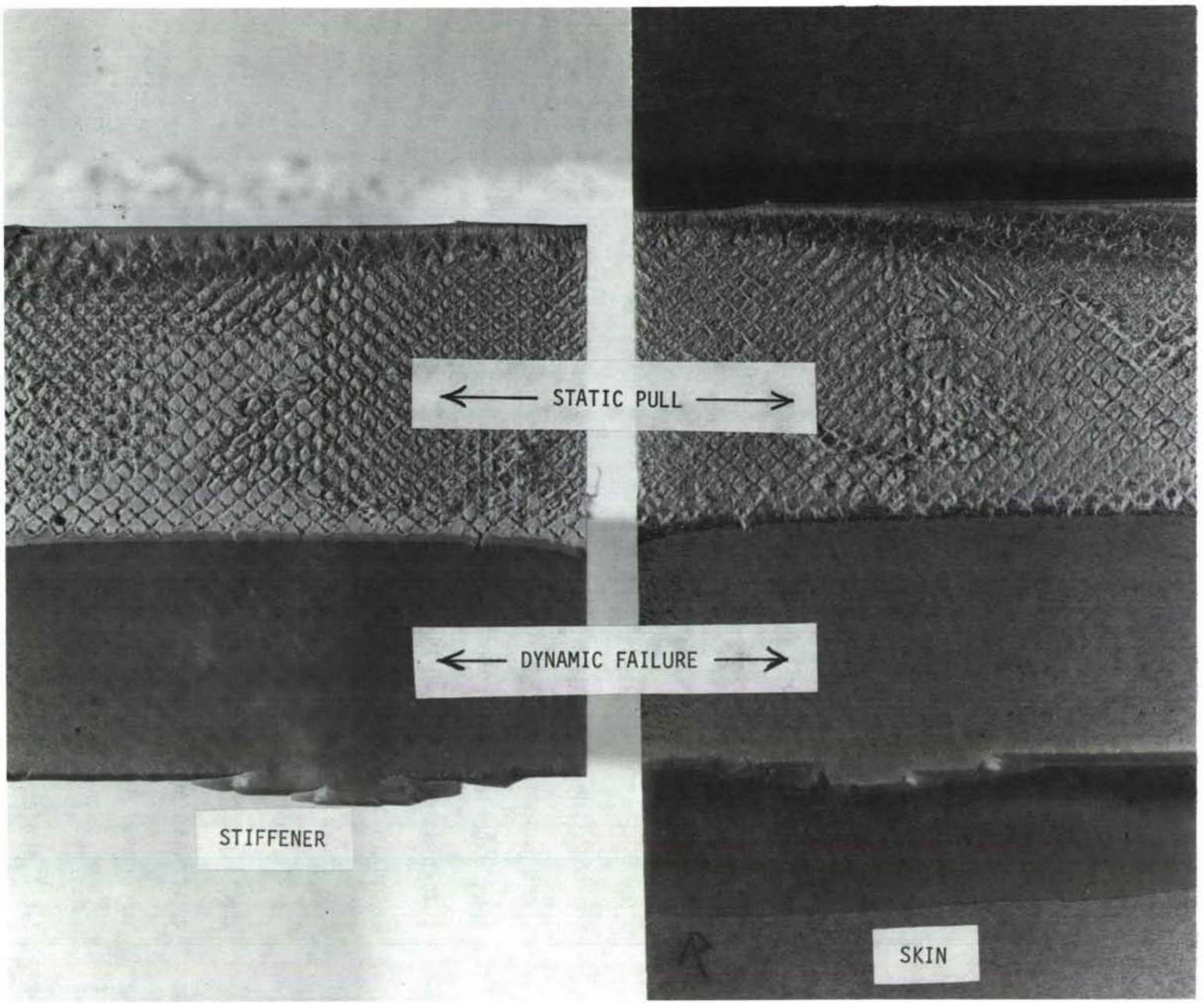

Figure Nr. 1 - Surfaces of Bonded Joint after Failure

SECTION IV

FATIGUE TESTS

1. DESCRIPTION OF TEST SPECIMENS

The baseline materials and procedures used in this investigation represent those used in the Air Force "PABST" program with Douglas Aircraft Company. In the "PABST" program, a section of a fuselage structure of a transport aircraft was designed, fabricated and tested. The generic design of the PABST structure consisted of tees and longerons adhesively bonded to the skin with frames mechanically fastened to the tees. The skin was 2024 T-3 (bare), the tees 7075 T-6 (bare), the surface treatment phosphoric acid anodize and the adhesive/primer system FM73/BR127. The FM73 adhesive is a nitrile rubber modified epoxy film and the primer consists of an epoxy phenolic resin in organic solvent with particulate inorganic chromate as the corrosion inhibitor. The baseline skin/tee specimens used in this investigation (Group A) used these same materials and processes. Also, the same specific values for important material and process parameters, such as primer thickness, adhesive layer thickness and surface preparation were used. The test specimens were fabricated in the AFWAL Materials Laboratory. The dimensions of test specimens are shown in Figure 2.

In addition, three groups of specimens (Group B, C, and D) were fabricated, using the "PABST" material and process technology, but with the primer thickness and adhesive layer thickness different from those used in the PABST program. A fifth group of specimens (Group E) was fabricated using the FM73/BR127 adhesive/primer system, but with Forest Product Laboratories' (FPL) etch surface treatment instead of phosphoric acid anodize. A sixth group of

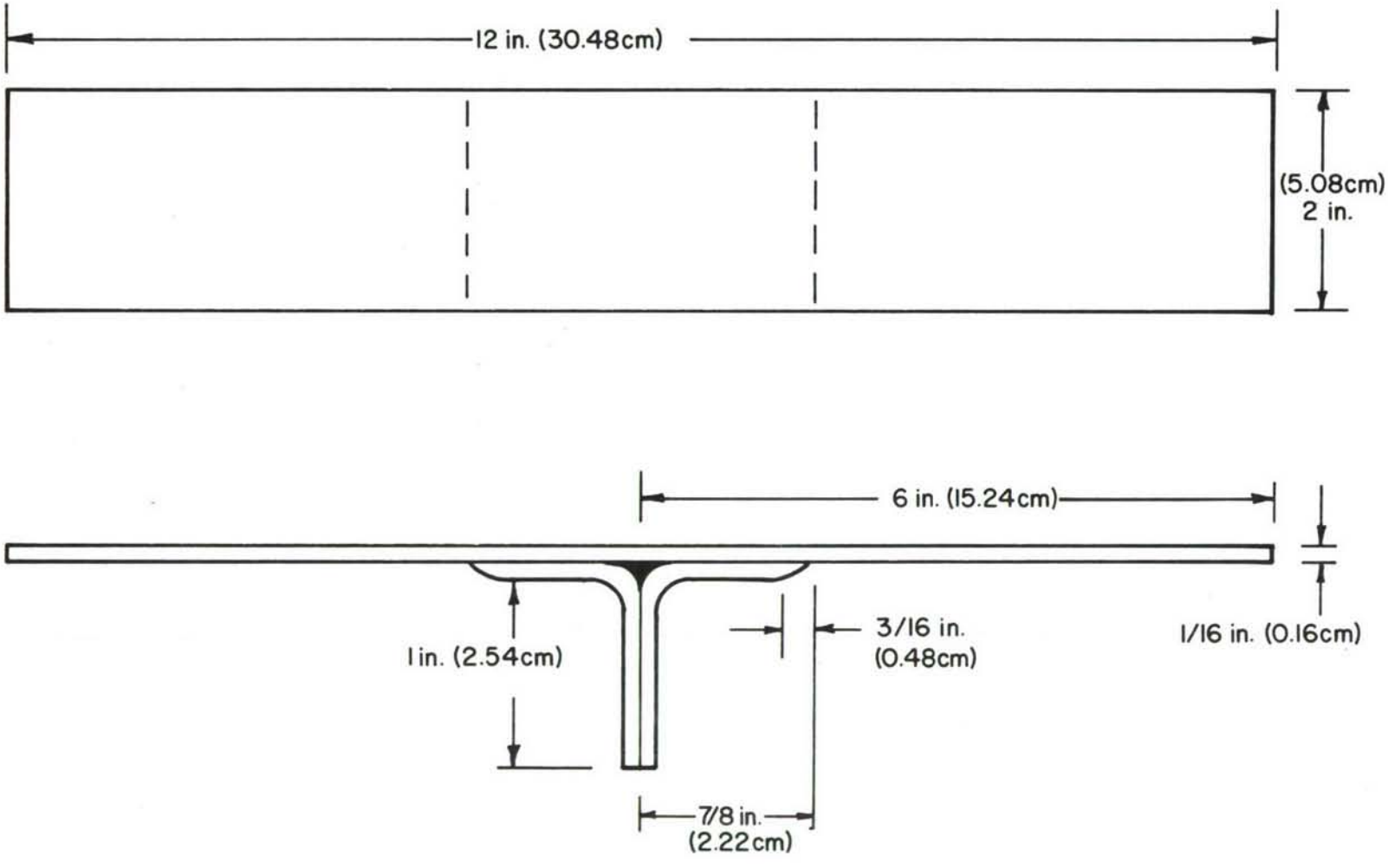

Figure Nr. 2 - Dimensions of Beam Coupons

specimens (Group F) was fabricated using the AF30/EC1660 adhesive/primer system, which is a nitrile rubber phenolic type. A listing of the six sets of specimens, showing the adhesive/primer type, adhesive thickness, primer thickness and surface treatment used, is shown in Table I. Three specimens per group were prepared and tested, making a total of eighteen specimens.

TABLE I
BONDED ALUMINUM COUPON NUMBERS

GROUP NUMBER	DESIGNATION OF ADHESIVE/PRIMER	CURED ADHESIVE LAYER THICKNESS INCHES (CM)	PRIMER THICKNESS INCHES (CM)	SURFACE PREPARATION	
				PHOSPHORIC ACID ANODIZE	FPL ETCH
A	FM73/BR127 (1)	.007 (.018)	.0003 (.00076)	X	
B	FM73/BR127 (1)	.007 (.018)	.0001 (.00025)	X	
C	FM73/BR127 (1)	.026 (.066)	.0001 (.00025)	X	
D	FM73/NONE (1)	.008 (.020)	NONE	X	
E	FM73/BR127 (1)	.007 (.018)	.0001 (.00025)		X
F	AF30/EC1660 (2)	.010 (.025)	.0003 (.00076)		X

(1) PRODUCT OF AMERICAN CYANAMID CO.

(2) PRODUCT OF 3M CO.

The reason for investigating variations in the FM73/BR127 system was to determine to what extent they influenced the initiation and propagation of interfacial and cohesive fracture. The AF30 adhesive was selected in this program as an adhesive having a lower modulus of elasticity and higher strain-to-fracture than FM73 adhesive. It was anticipated that these characteristics might make it more suitable to withstand the oscillating peel stresses caused by acoustic loads.

The first step of processing and fabrication was to surface treat the adherends using specification BAC5555 for the phosphoric acid anodize and BAC5514 for the FPL etch. Then, primer was applied from a nitrogen pressurized spray gun, air dried and heat cured. After film adhesive was laid between the tee flange and the skin, the assembly was enclosed in a vacuum

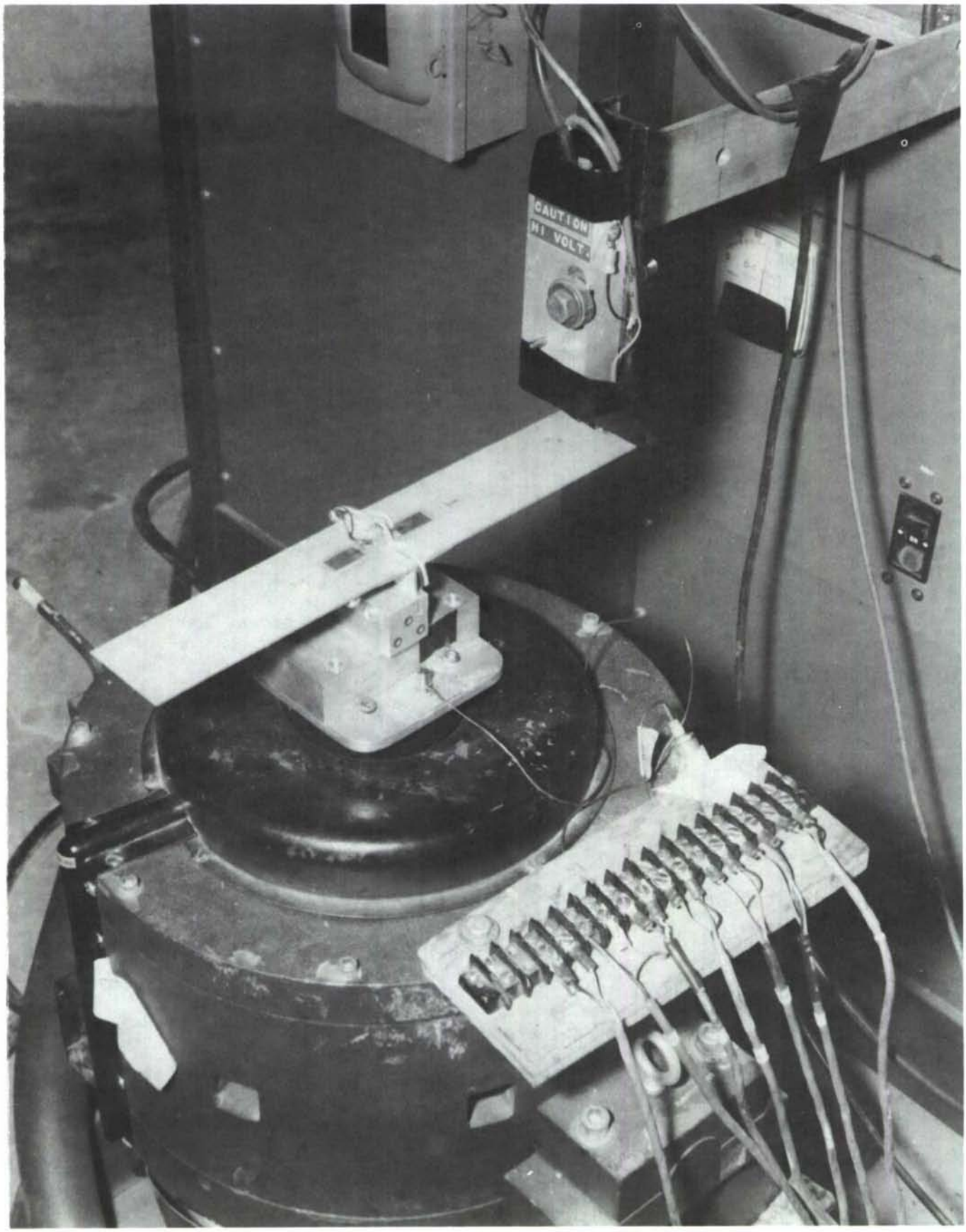

Figure Nr. 3 - Test Coupon Mounted on Vibration Shaker

bag and cured in an autoclave according to the adhesive manufacturer's recommended cure cycle. Detailed information on processes and fabrication procedures are given in the Appendix.

Two measures were taken in order to assure the quality of the fabricated specimens. One was to fabricate companion lap shear and wedge test panels, along with the skin/tee panels, for subsequent tests. The other was to perform nondestructive inspection of the bondline of the skin/tee specimens using ultrasonic attenuation and X-ray.

The lap shear specimens, tested at room temperature, met the strength requirements. The wedge specimens, exposed to 140° F (60°C) at 100% relative humidity, met the crack extension requirements, except for Groups B and C. These specimens had a lower primer thickness than normal. This behavior was anticipated, since the primer thickness was about half that considered acceptable from a durability standpoint. However, as this program was to investigate the primer thickness for its effect on structural behavior rather than durability, the poor wedge test results were not considered a basis for rejecting the skin/tee specimens for fatigue testing. The ultrasonic and x-ray inspections of the bondlines did not reveal any significant flaws or anomalies in any of the skin/tee specimens.

2. TEST PROCEDURE

All phases of the test program were conducted on an in-house basis using the test facilities and data reduction capabilities of the Flight Dynamics Laboratory. The double cantilever beam coupons were clamped at the midspan stiffener on an electromagnetic shaker as shown in Figure 3. The supporting test equipment and instrumentation are shown in Figure 4 and block-diagrammed in Figure 5. A low level frequency sweep was made of each coupon to determine its resonant frequency. Damping measurements were accomplished using the log

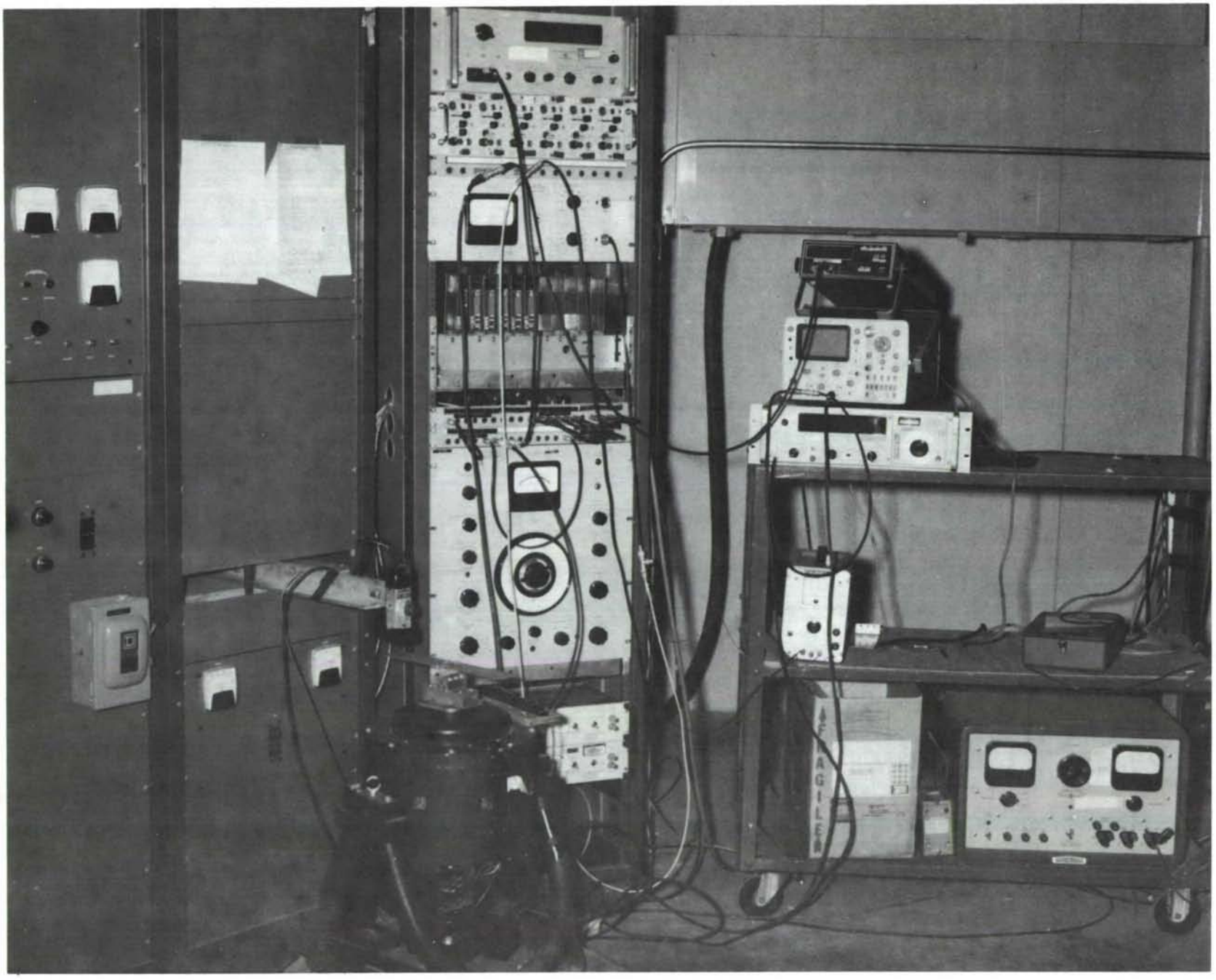

Figure Nr. 4 - Overall View of Test Equipment and Instrumentation

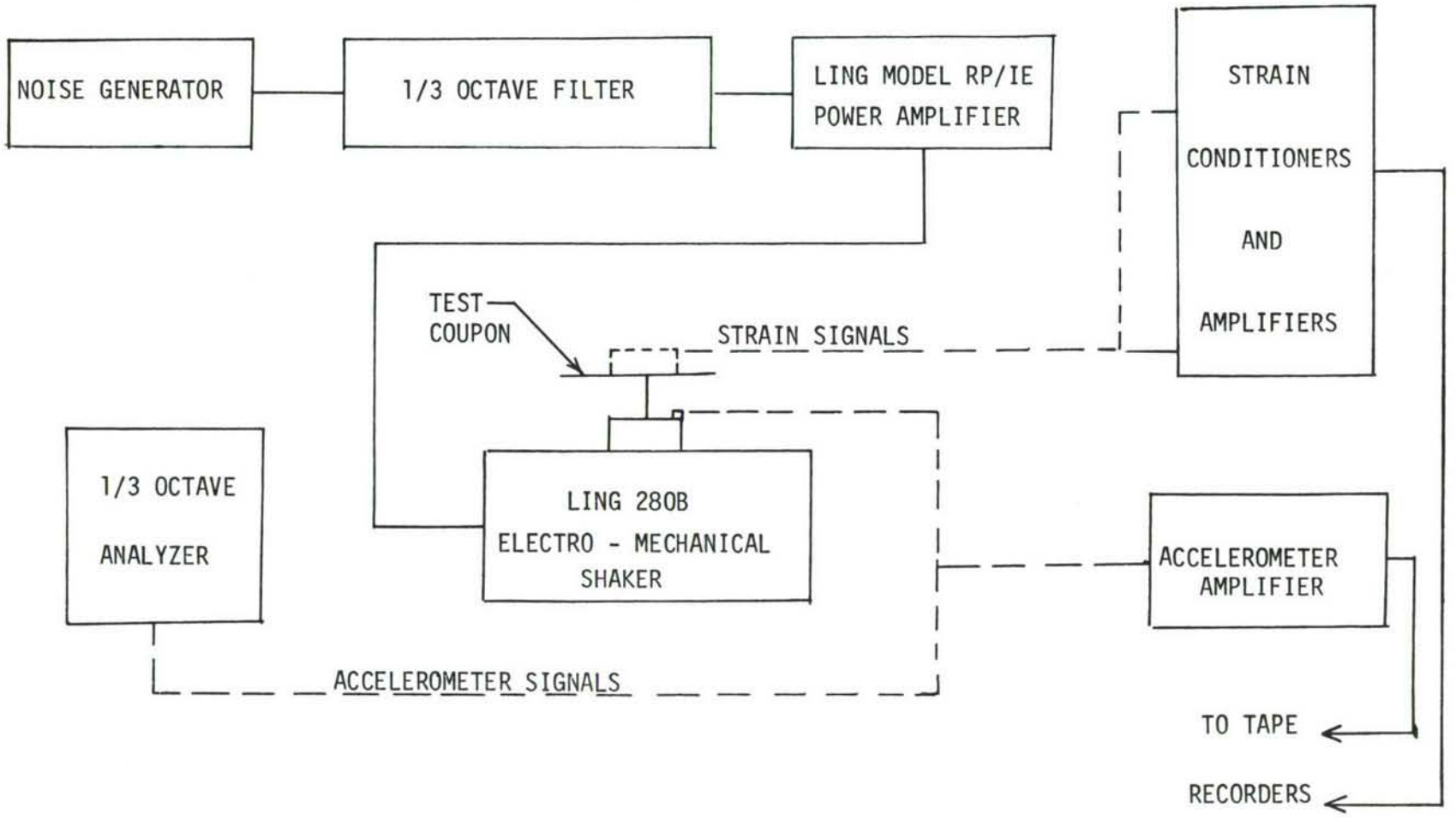

Figure Nr. 5 - Block Diagram of Instrumentation

decrement method. This technique depends upon measuring the amplitude rate-of-decay of the coupon vibrating at its fundamental resonant frequency after abruptly cutting-off the exciting force. The damping ratios (C/C_c) for each of the six coupon groups are summarized in Table II. The five groups (A, B, C, D, E) using FM73 adhesive all have damping ratios that are comparable, ranging from 0.00086 to 0.00121. The exception is Group F, using the more pliable AF30 adhesive, which makes a noticeably "softer" bonded joint, with a corresponding increase in damping ability. This is reflected in the higher damping ratios for the AF30 adhesive which averaged 0.0165. It should be noted that the damping ratios for riveted structure usually fall within the range found with the FM73 adhesive.

TABLE II

BONDED COUPON DAMPING FACTORS

Coupon Number	C/C_c	Coupon Number	C/C_c
A-1	.00087	E-1	.00094
A-3	.00086	E-2	.00088
B-1	.00121	E-3	.0011
B-3	.00092	F-1	.0156
C-1	.00106	F-2	.0172
C-2	.00098	F-3	.0169
C-3	.00097		
D-1	.00097		
D-2	.00096		
D-3	.00099		

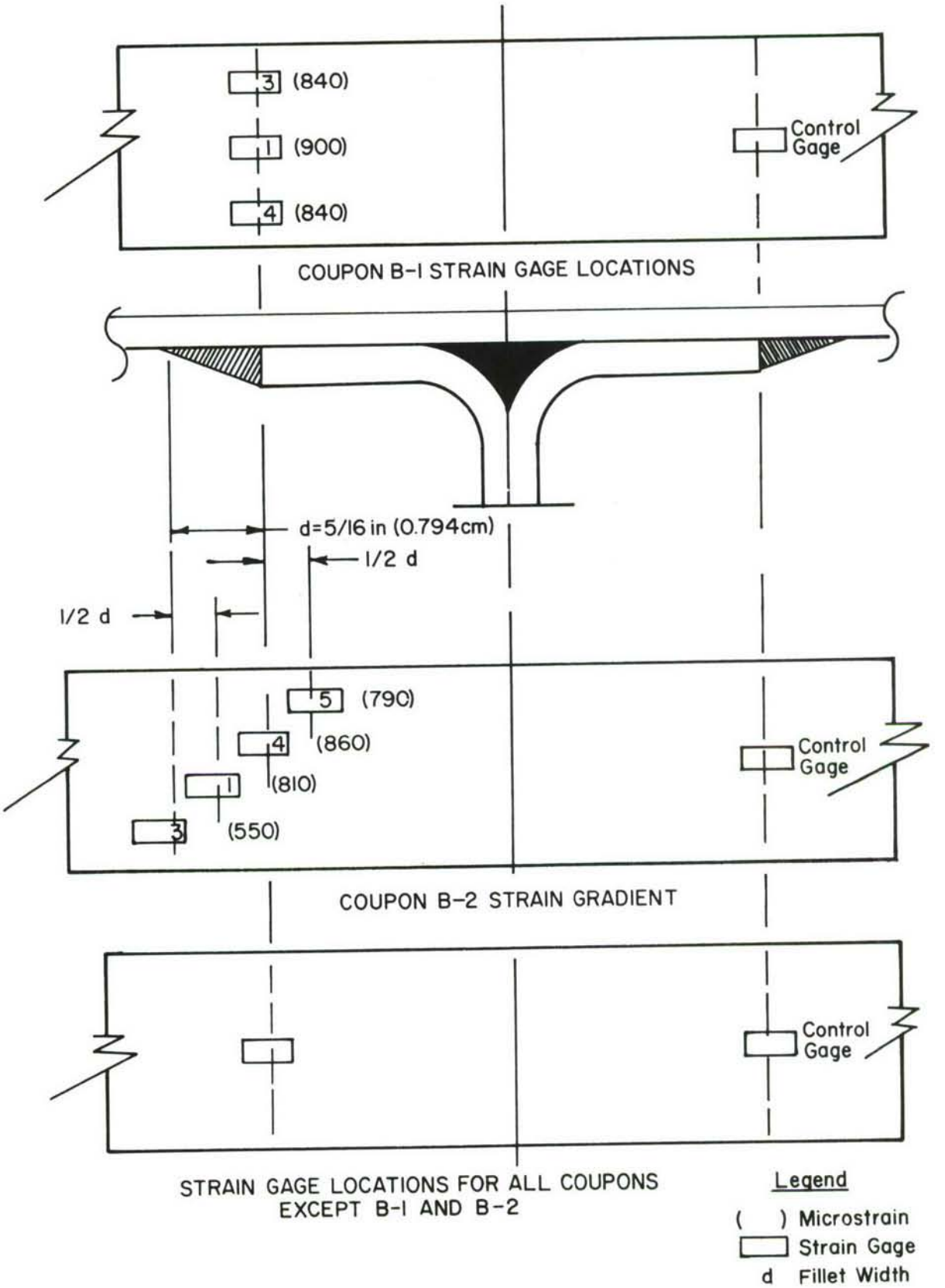

Figure Nr. 6 - Strain Gage Locations on Test Coupons

Preliminary strain measurements were made prior to fatigue testing for two reasons. First, strains were recorded on Coupon Nr. B-1 to determine whether torsional side loads were present in the shaker drive system that might adversely affect the bending fatigue data. Three gages were used as shown in Figure 6. The resulting strain readings are listed in parentheses next to each gage position. The strain readings differed by only 60 microstrain on either side of the center gage, indicating that no torsional effects of any significance were present.

It was also necessary to verify where the maximum bending strain occurs on the coupon. This would determine where to install the control gage during fatigue testing. Since the strain usually is expected to peak at or very near the edge of the stiffener, the precise location of each strain gage is critical for an accurate measurement of the strain distribution. Therefore, four strain gages were installed on coupon number B-2, as shown in Figure 6. To further improve the accuracy of the measurements, it was advantageous to use a gage that senses the strain over as small an area as practical. BLH type DLB-PT12-2A wire strain gages were used that have a 1/8 inch grid length. The resulting strain gradient is plotted in Figure 7, showing that the peak strain was recorded by the gage centered on the edge of the stiffener. Accordingly, the control gages on the remaining coupons were located at the same place.

The coupons were vibrated at resonance to generate alternating bending stresses in the beam until failure was observed. A failure was defined either as a separation in the bonded joint or as a skin crack that was visually detectable without magnification. During stabilized fatigue test conditions,

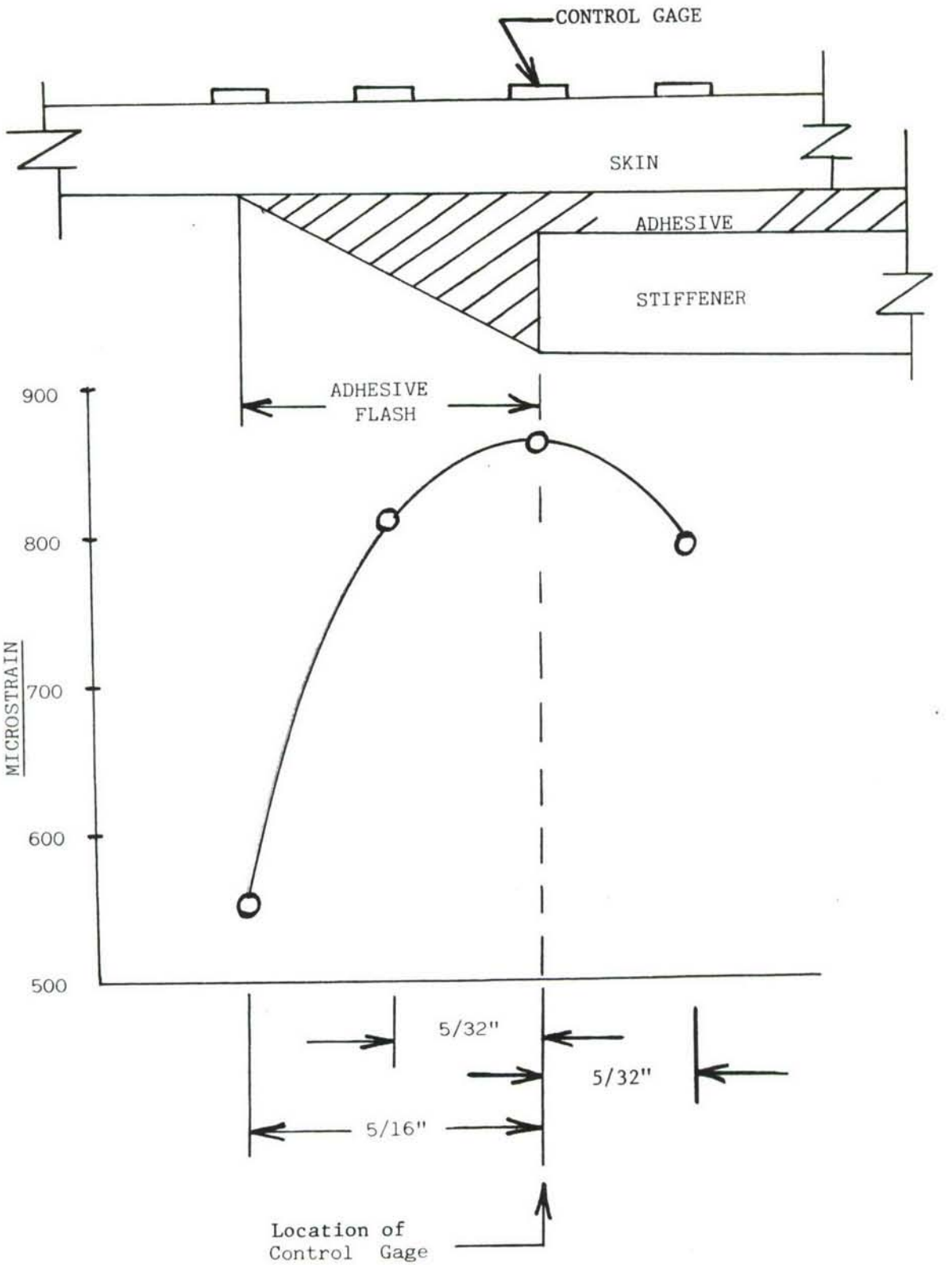

Figure Nr. 7 - Strain Gradient Across Coupon Bond Line

the shaker drive acceleration (input) and the coupon strain levels (output) were recorded on tape. Typical examples of these data are shown in Figures 8 and 9.

A baseline strain level of 900 microstrain was selected for all coupons to provide a comparison with data from previous programs where tests were conducted at the same level. Whenever feasible, each specimen was fatigue tested in second-mode bending to enable the accumulation of stress cycles at a much higher rate than possible in the first mode. There were two exceptions to this during the testing. In one instance, the shaker acceleration capability was not sufficient to drive the Group F nitrile phenolic coupons in the second mode at the required stress level of 900 microstrain. This was attributed to the "soft" skin-stiffener joint resulting from the AF30 adhesive which is more pliable than the FM73. Consequently, the Group F coupons were tested at their fundamental frequency, which required considerably less shaker head acceleration to attain 900 microstrain. The test results are summarized in Table III. All three coupons that comprised Group B experienced identical skin failures near mid-span. Since no failures were evident in the adhesive, the test was continued by cutting-off both ends of each Group B coupon. The resulting beams, 3-3/4 inches long (9.525 cm) were tested in the first mode until failure was induced. These are identified as Group B-M (modified).

Failure time was determined from visual inspection of each test coupon conducted at 2 to 3 hour intervals, or whenever the coupon response frequency showed a noticeable decrease. When this point was reached, the test was terminated and the time to failure recorded. Figure 10 shows typical time histories of the frequency response. The exact time of crack initiation is not evident from these plots. The change in the slope of the frequency

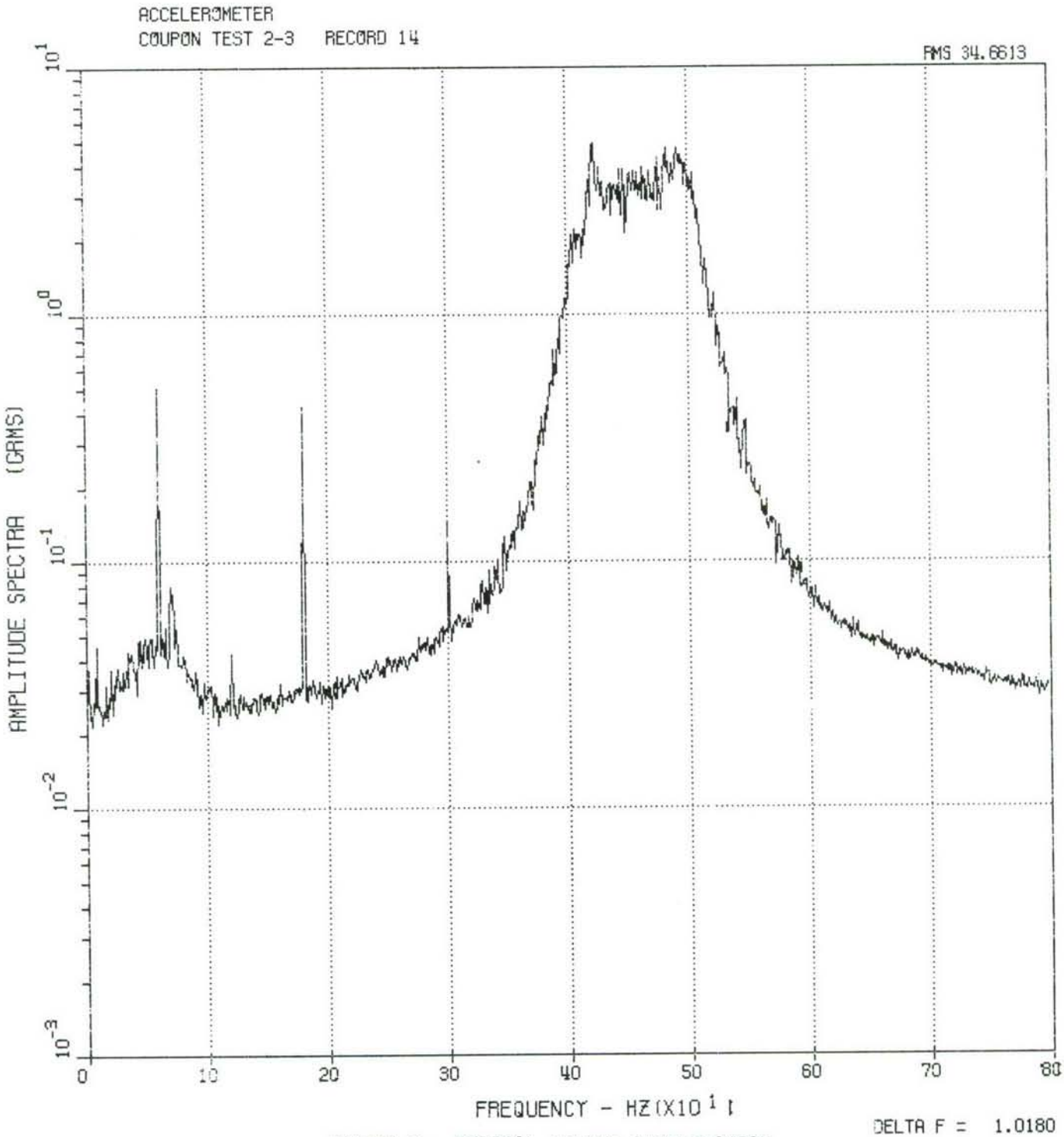

FIGURE 8 - TYPICAL SHAKER ACCELERATION

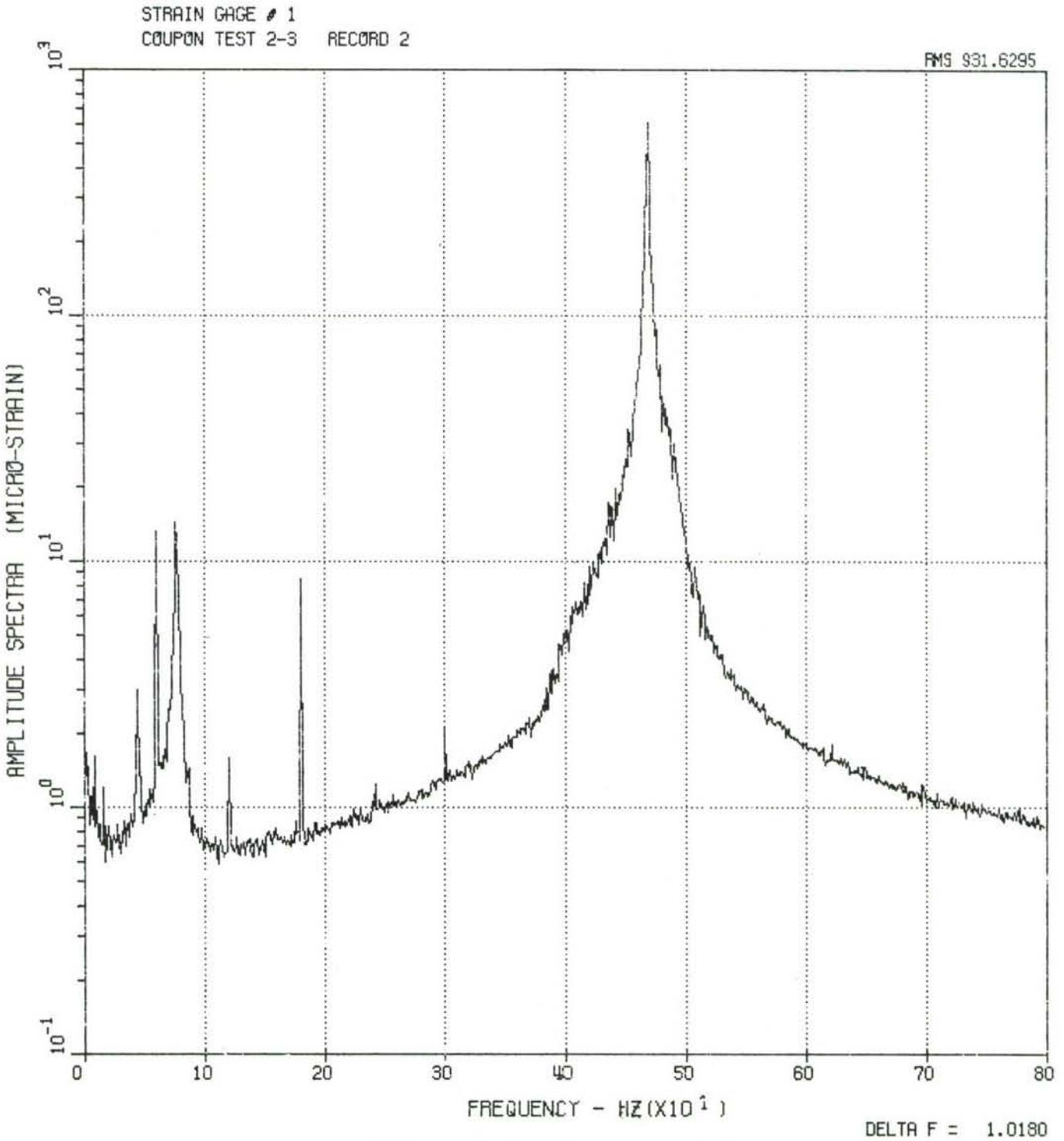

FIGURE 9 - TYPICAL STRAIN RESPONSE

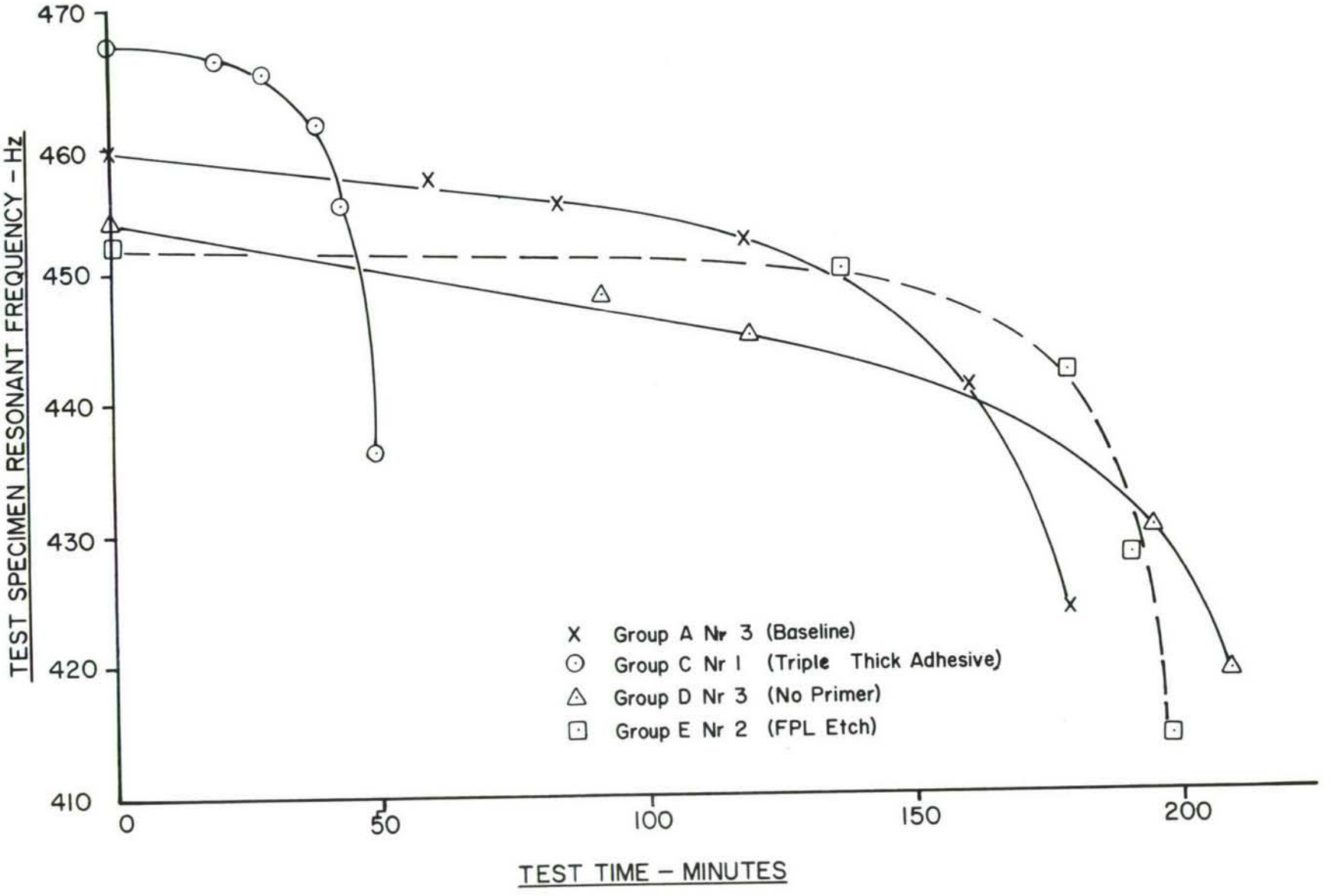

Figure Nr. 10 - Change in Resonant Frequency vs Time

TABLE III

SUMMARY OF BONDED ALUMINUM COUPON FATIGUE TEST DATA

900 MICROSTRAIN

COUPON GROUP-NR	FREQUENCY HZ	SHAKER HEAD ACCEL G'sRMS	FAILURE TIME MINUTES	CYCLES TO FAILURE X 10^6	TYPE OF FAILURE
A-1	456	24	171	4.68	Adhesive Bond
A-2	456	--	98	2.68	Stiffener
A-3	459	26	179	4.93	Adhesive Bond
B-1	448	28	170	4.57	Mid-span Skin
B-2	450	31	308	8.32	Mid-span Skin
B-3	450	--	172	4.64	Mid-span Skin
B-M-1	127	10	+164	5.82	Skin
B-M-2	162	11	+418	12.38	Adhesive
B-M-3	143	11	+444	8.45	Skin
C-1	436	31	49	1.28	Adhesive Bond
C-2	468	31	69	1.94	Adhesive Bond
C-3	468	--	98	2.75	Adhesive Bond
D-1	455	29	158	4.31	Skin
D-2	453	27	163	4.43	Skin
D-3	453	29	208	5.65	Skin and Adhesive Bond
E-1	452	29	226	6.13	Skin
E-2	452	--	211	5.72	Skin
E-3	452	28	418	11.34	Mid-span skin/Adhesive
F-1	69	17	710	2.94	Adhesive Bond
F-2	70	17	1104	4.64	Adhesive Bond
F-3	69	18	661	2.74	Adhesive Bond

response versus time with the same bending load was not consistent. The beam coupons with the thicker adhesive failed much sooner. The resulting failure times are summarized in Table III. The cycles to failure were obtained by multiplying the failure time by the modal frequency. Group B coupons failed at the midspan of the beam and were classified as skin failures. Further testing produced skin failures in two coupons and adhesive failure in the third. A total of seven skin failures and 11 adhesive bond failures were obtained during this program. Most of the failures fell with 10^6 to 10^7 cycles. This scatter is normal for coupon testing at the same RMS strain. The beam coupons with the thicker adhesive had somewhat shorter fatigue lives. Changes in the surface preparation and primer thickness did not produce a significant change in the fatigue life.

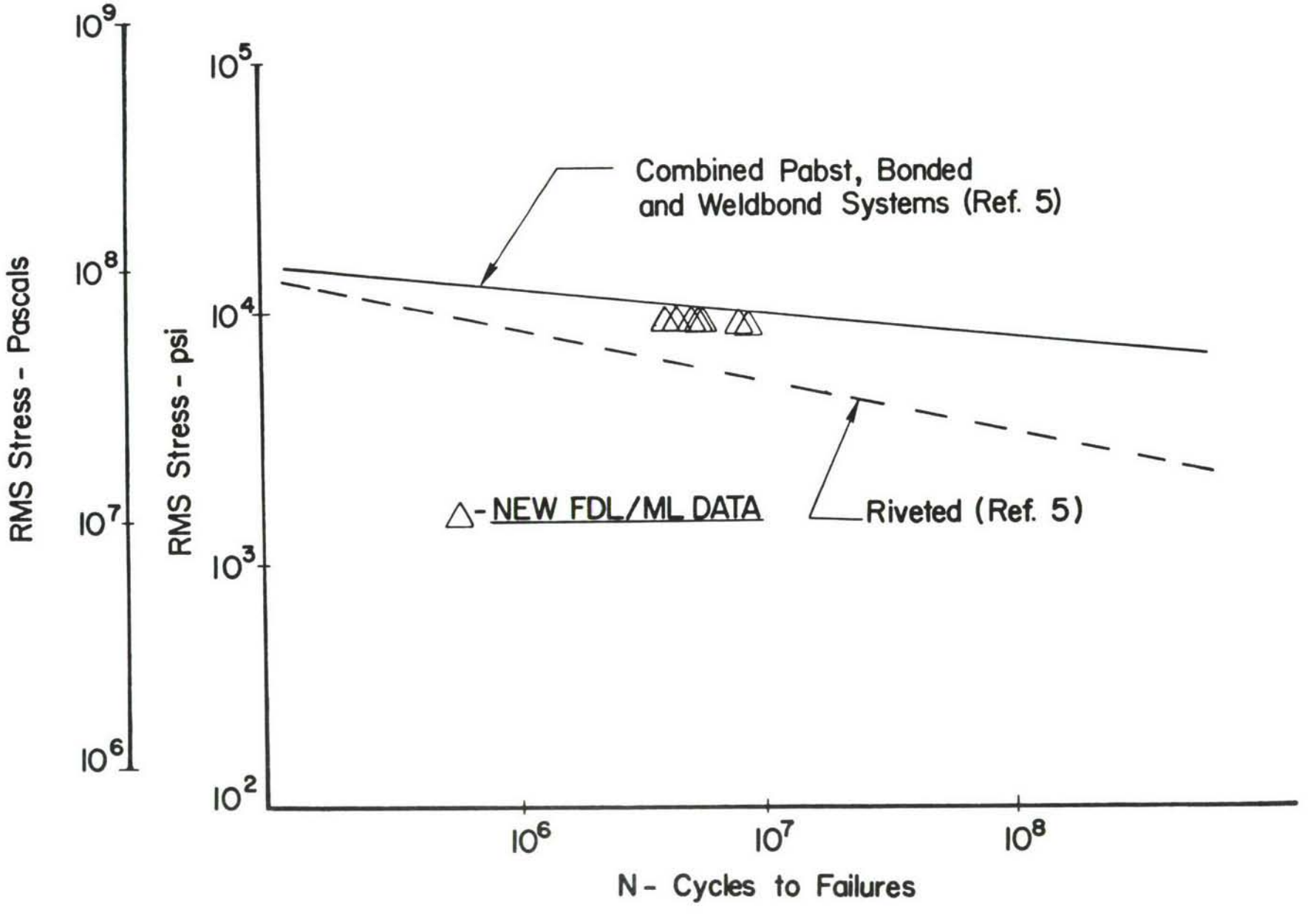

Figure Nr. 11 - Comparison of FDL/ML Skin Failures with Previous Test Data

Since conclusions drawn from a small number of fatigue failures can be misleading, these data were compared with the results from previous investigations and are identified herein as FDL/ML data. The skin failures are plotted in Figure 11 and compared very closely with the S-N curve developed in Reference 5.

The time-to-failure of the adhesive in a bonded joint not only is a function of the strain in the surface of the coupon, but of the coupon thickness. Therefore, in previous investigations[5] the strain data were converted to bending moment data to develop M-N (Bending Moment-Cycles to Failure) curves which account for variations in beam thickness. Computing the bending moments from the strain permits the data to be presented on one curve for all thicknesses. The following relationship was used to determine the bending moment:

$$\overline{M} = S\ E\ \overline{\epsilon}$$

where $\overline{M}$ = RMS bending moment
S = Section modulus
E = Young's modulus
$\overline{\epsilon}$ = RMS bending strain

Figure 12 shows the 11 new adhesive fatigue failures (FDL/ML data) compared to previous data obtained from FM73 and AF55 adhesives. The dashed lines were constructed through the outlying points of the previous data and are parallel to the previously established M-N curve. Most of the new data fell within these outliers established from the data. A new M-N curve was then constructed from the FDL/ML data through the average value of the fatigue failures and parallel to the previous M-N curve. For a given moment, an increase in life by a factor of approximately 20 can be expected using the M-N curve developed with the FDL/ML fatigue failures.

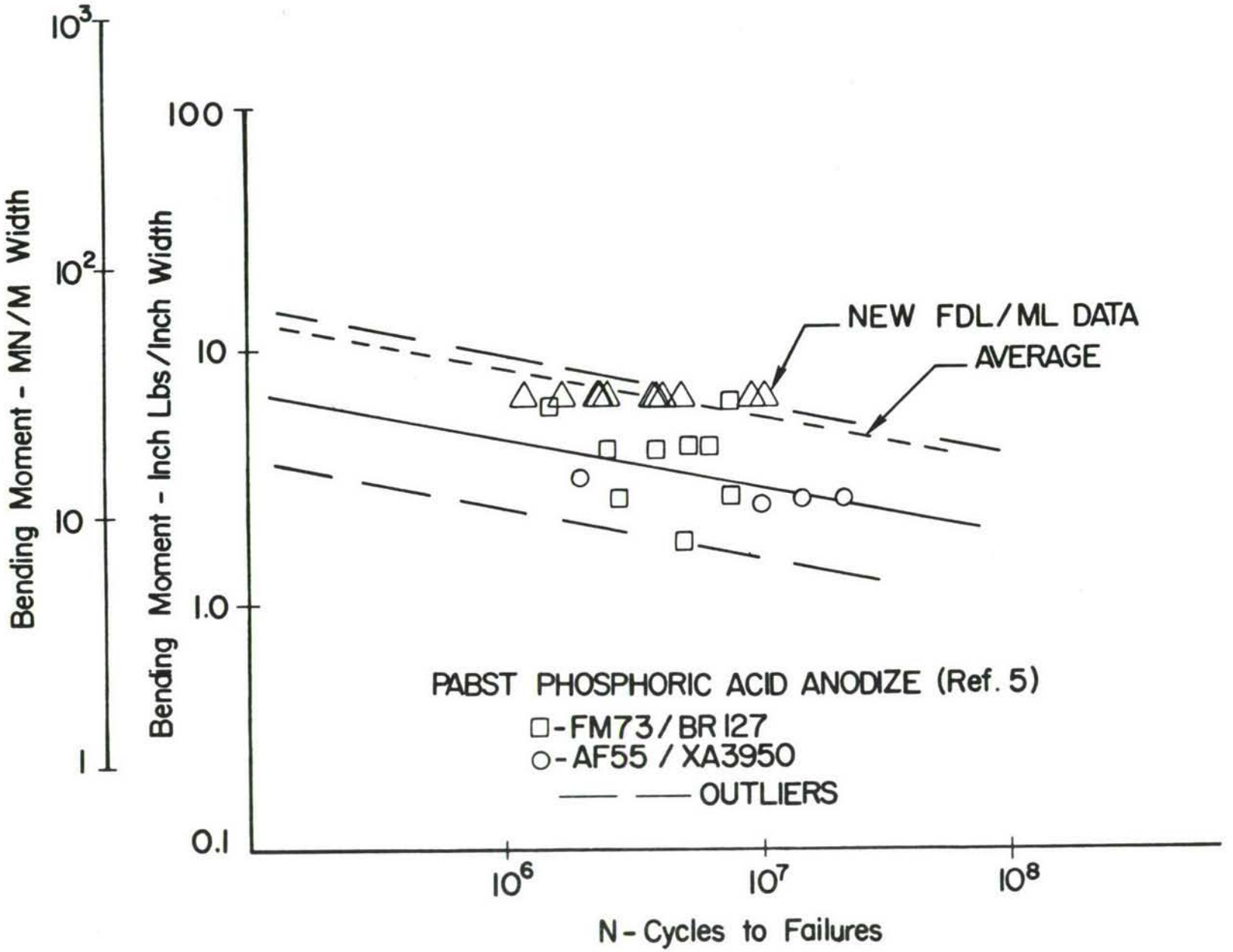

Figure Nr. 12 - Comparison of FDL/ML Bond Failures with PABST Data

Figure 13 shows the 11 new adhesive fatigue failures compared with previous data from FM137 adhesive and metal bond etch surface preparation. Fatigue failures with the adhesives used in FDL/ML beam coupons occurred at a higher load than the FM137. The FM137 data produced a very flat M-N curve.

Figure 14 shows the FDL/ML data and the M-N curve developed using the combined PABST, baseline bonded and weldbonded data.[5] The M-N curve for the FDL/ML data was constructed through the average value of the fatigue failures and parallel to the previous combined curve. For a given bending moment, it is shown that an increase in life by a factor of approximately 30 can be expected with the M-N curve developed with the FDL/ML fatigue failures.

The shaker beam tests determined the life of the bonded joint for each adhesive at a particular strain level on the surface of the beam. While the fatigue life for the more pliable AF30 coupon at 900 microstrain was comparable with FM73, a much higher excitation force was required to produce the same strain in the AF30 coupon for the same excitation mode. Therefore, if an acoustic test were conducted with panels fabricated using these two adhesives at the same sound pressure level, it is expected that the skin stresses in the panel fabricated with the AF30 adhesive would be much lower. This decrease in the skin stresses would increase the sonic fatigue life of the structure. The damping data obtained from the AF30 coupons indicated a significantly higher damping ratio than from the FM73 adhesive. This also tends to increase the sonic fatigue life.

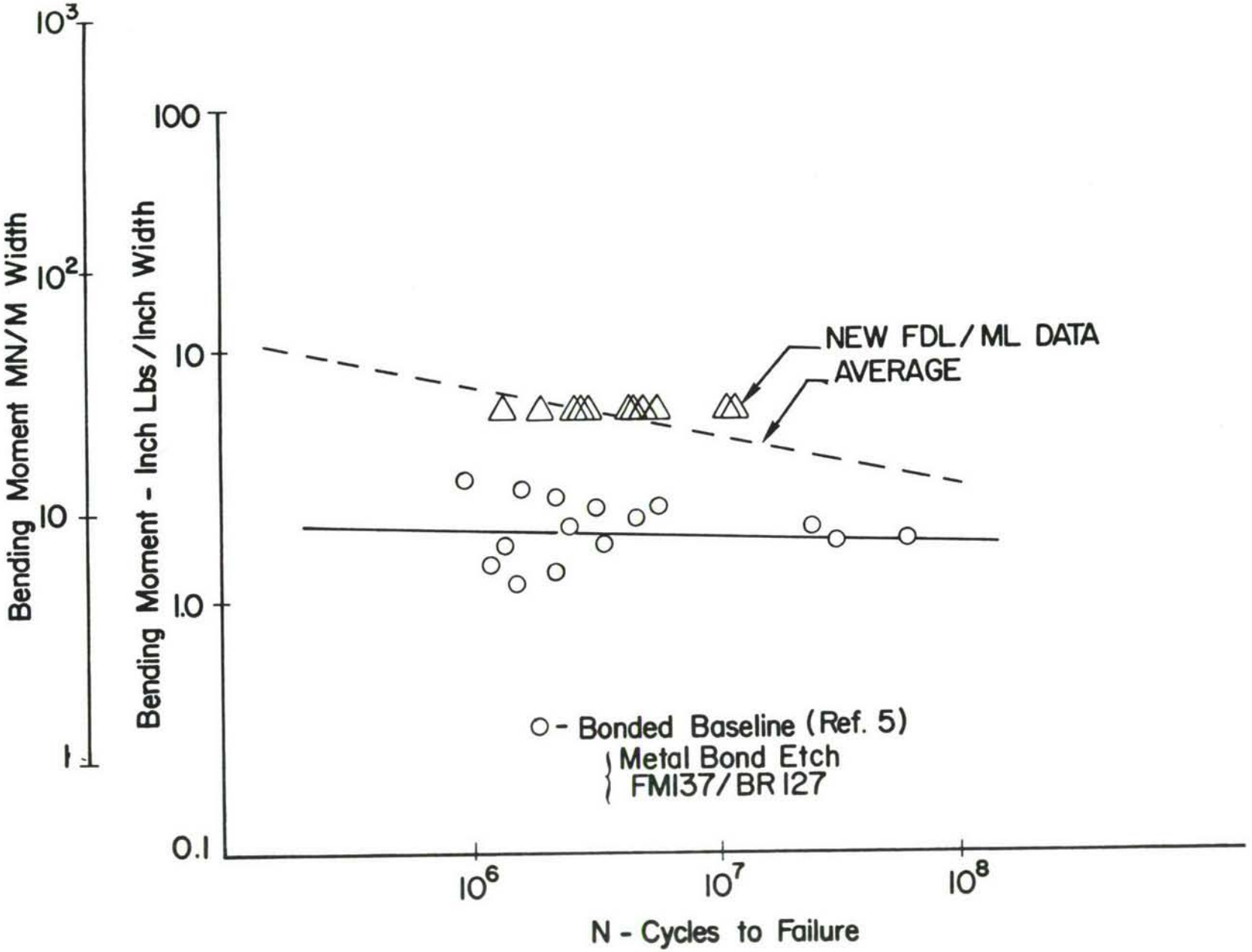

Figure Nr. 13 - Comparison of FDL/ML Bond Failures with Bonded Baseline Data

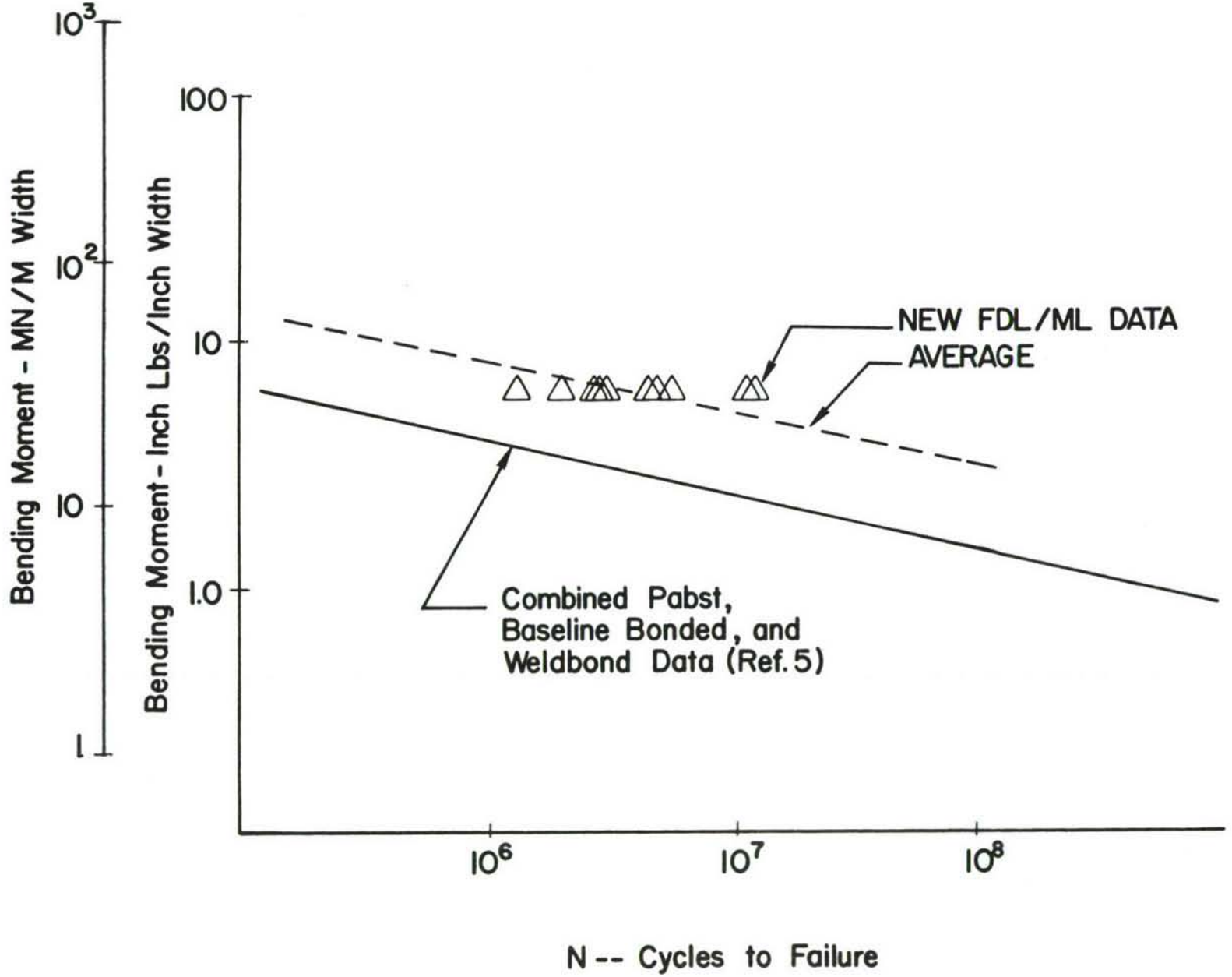

Figure Nr. 14 - Comparison of FDL/ML Bond Failures with Combined PABST, Baseline and Weldbond Data

SECTION V

FRACTOGRAPHIC ANALYSIS OF TEST SPECIMENS AFTER FAILURE

After each specimen had been fatigue tested, the propagation of the debond from the edge of the tee flange inward was typically about 3/8 inch deep. It was decided to perform fractographic investigations, using a scanning electron microscope (SEM) on the fracture surfaces which had debonded during testing.

To accomplish this, it first was necessary to separate the remaining bonded area of the specimen without changing the character of or contaminating the initial fracture surface. A file mark was made on the edge of the specimen where the fatigue fracture appeared to stop to clearly differentiate that part of the fracture surface created during fatigue testing from the part created by cleaving the remaining bonded portion. The specimen was then immersed in liquid nitrogen for several minutes and the remaining bond was pried apart. This was done by gripping the upstanding leg of the tee and the portion of the skin beyond the bonded area to make sure the fracture surfaces were not touched. This procedure avoided excessive deformation of the adherends since the adhesive became brittle enough to readily cleave. The mating fracture surface portions of the specimen from both skin and tee were cut off and prepared for SEM examination by vacuum coating with carbon. One representative specimen from each of the six groups was used in the fractographic investigations.

The objectives of the fractographic investigations were to determine the locus of fracture and the fracture mechanism. The preferred locus of fracture is cohesive (totally within the adhesive layer) because this type of fracture

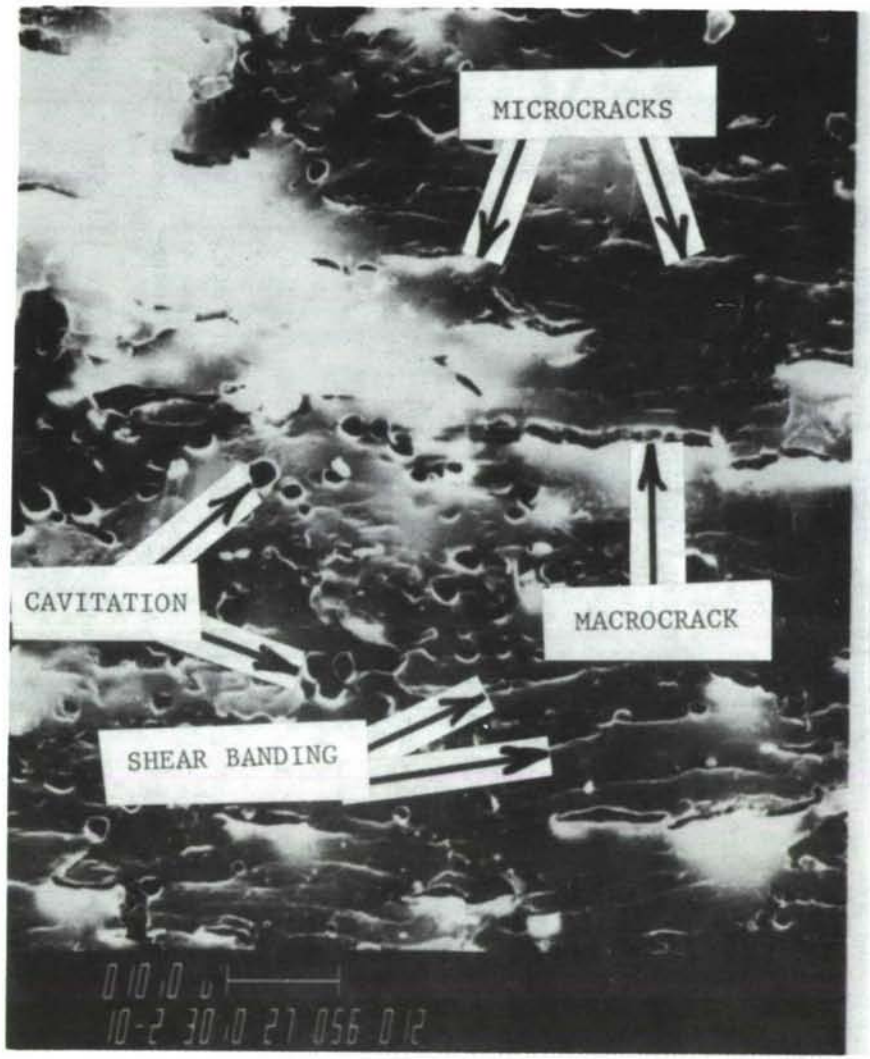

Figure Nr. 15 - Example Photomicrograph of Adhesive Failure

Figure Nr. 16 - Example of Photomicrograph of BR127 Primer Layer

is predictable from measurable properties of the adhesive. In actual practice, fractures can also occur within the primer or the aluminum oxide layer or at the adhesive/primer, primer/oxide, or oxide/aluminum interfaces.

The adhesives, primers and oxide layers investigated in this program have distinct morphological features which are easily distinguishable in the scanning electron microscope. Therefore, the determination of locus of fracture was a relatively straightforward matter. For example, the FM73 adhesive is a two phase material, consisting of elastomeric particles (precipitated during the curing reaction) in an epoxy continuum. Under combined shear and tensile loading such as the adhesive was subjected to in the fatigue tests, the adhesive fractures by cavitation around the elastomeric particles and by "shear banding," which has the appearance of thin layers, displaced stepwise from each other. Under repetitive loading or increasing magnitude of load, cracks form around these cavities, the cracks coalesce together forming macrocracks, and then gross fracture occurs. An example of such "cohesive" fracture is shown in Figure 15.

The BR127 primer, used in conjunction with FM73 adhesive, contains a chromate corrosion inhibitor in the form of needle-like crystals. This gives the primer layer (and interfacial regions incorporating the primer) a distinctive, easily recognizable appearance as shown in Figure 16.

The aluminum oxide surface can be recognized by grain boundaries and pitting in the surface as shown in Figure 17. This particular photomicrograph of the fracture surface of a primed adhesive bonded specimen shows a very thin layer of primer polymer adhering to the oxide surface. (This photomicrograph is of a fracture surface of a different adhesive/primer system from that investigated in this program and is included only to illustrate this specific type of fracture).

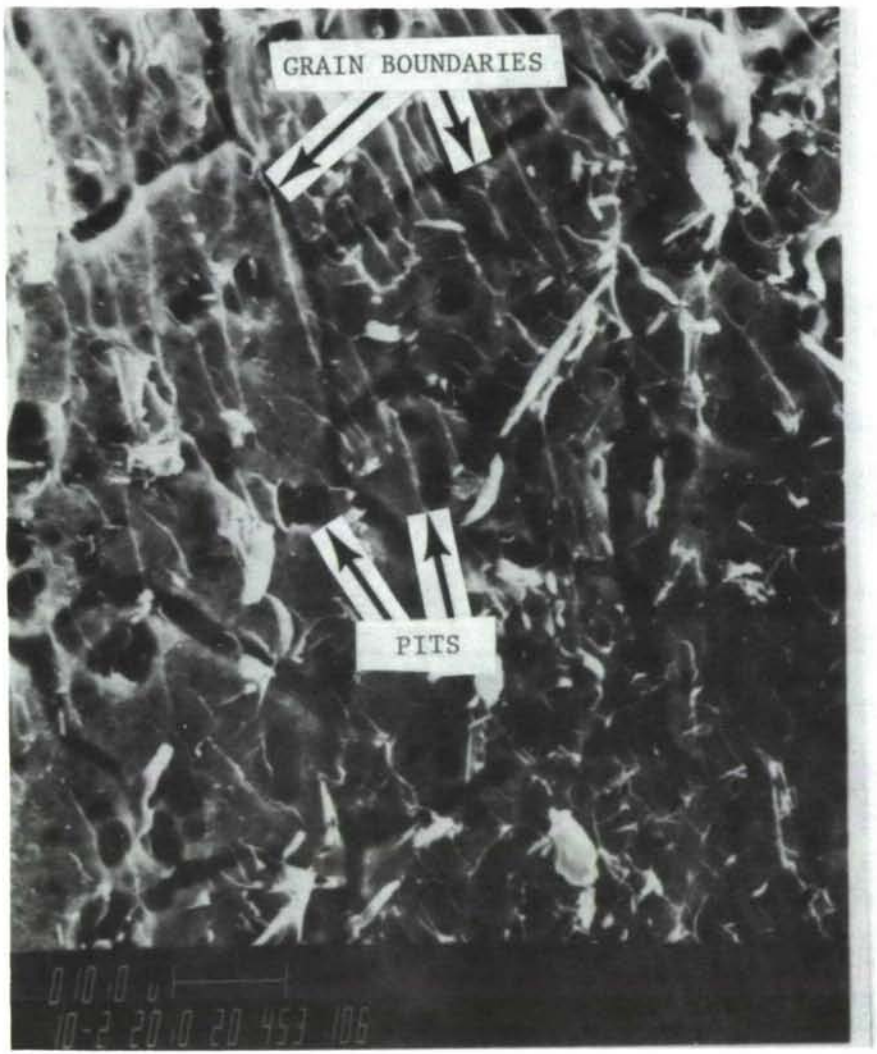

Figure Nr. 17 - Example Photomicrograph of Aluminum Oxide Surface

Figure Nr. 18 - Photomicrograph of "Fresh" Fracture Surface (Skin Side), Group A, Specimen Nr. 1

In addition to defining locus of fracture in the skin/tee specimens, the other objective of the fractographic investigations was to determine the "efficiency" of the fracture process. The term "efficiency" is used here to describe the degree to which the energy dissipation processes come into play during fracture. For example, combined cavitation, microcracking, and shear banding mechanisms for FM73 represent a high efficiency fracture process.

In observing the fracture surfaces of the skin/tee specimens, the fractures were predominantly cohesive and the fracture processes were efficient in that they involved multiple mechanisms. In some cases locus of fracture was very close to the primer but, even in these cases, there was still a thin layer of adhesive adhering to the primer. The following discussion describes features of representative photomicrographs made of the fracture surfaces.

For the standard PABST material system, (Group A Specimen Nr. 1) fracture was typically cohesive but very close to the primer on the tee. This was indicated from a series of photomicrographs of fracture surfaces, several of which are shown for illustrative purposes. Figure 18 shows the fracture surface of the skin side, clearly revealing the classical cavitation and shear banding typical of FM73 adhesive. There is little evidence of primer on the fracture surface except for small regions at the upper left and lower right. Figure 16 (previously referred to as illustrating a representative chromated primer surface) shows the mating fracture surface of the tee. The needle-like crystals of the chromate primer are very prominent. A thin layer of adhesive adhered to the primer, as clearly evidenced by the micro-cavitation in this layer. Therefore, the net conclusion was that fracture occurred in the adhesive very close to the primer on the tee.

The fracture shown in Figure 18 is immediately adjacent to a region which was intact (still bonded) when the fatigue test was terminated and, therefore,

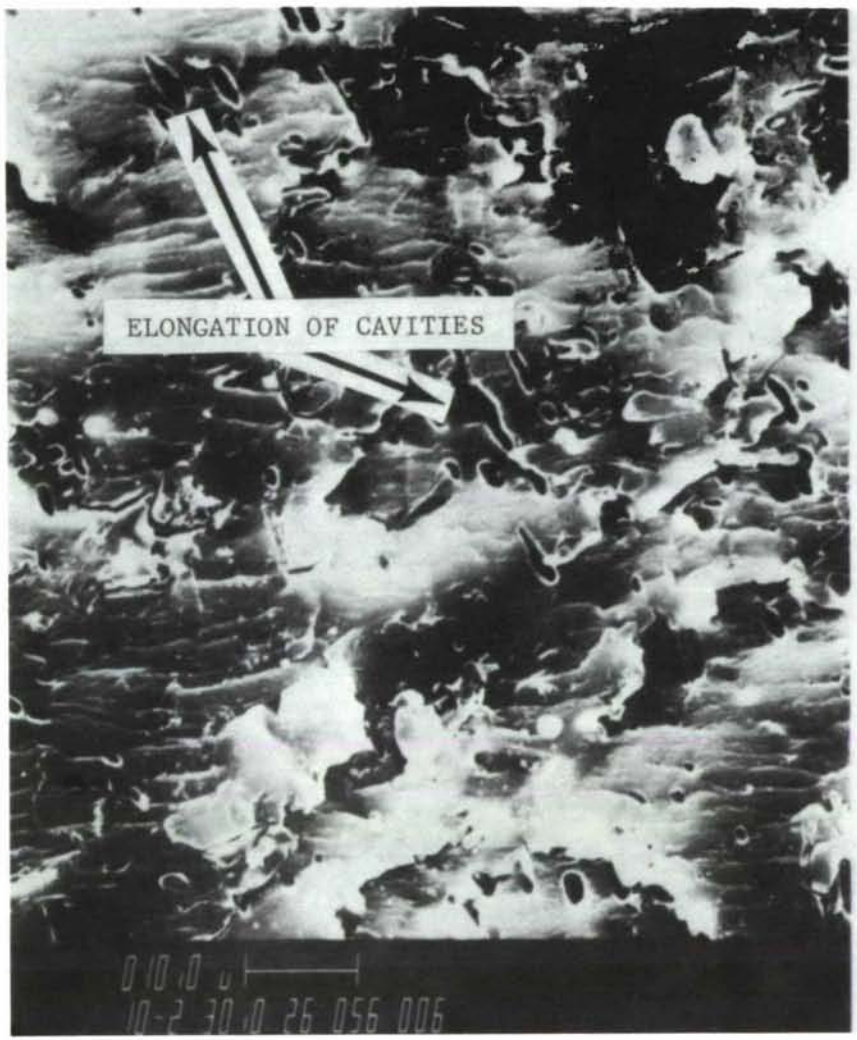

Figure Nr. 19 - Photomicrograph of "Early" Fracture Surface (Skin Side)
Group A, Specimen Nr. 1

Figure Nr. 20 - Photomicrograph of Fracture Surface (Tee Side), Group B, Specimen Nr. 2

Figure Nr. 21 - Photomicrograph of Fracture Surface (Skin Side), Group B, Specimen Nr. 2

Figure Nr. 22 - Photomicrograph of Fracture Surface (Tee Side), Group C, Specimen Nr. 2

represents a "freshly fractured" surface. The fracture surface in Figure 19 is about 1/8 inch (0.318 cm) further outboard (away from the tee) from that shown in Figure 18. Here, fracture occurred earlier since it was subjected to greater dimensional excursion. This caused elongation of the cavities and subsequent microcracks connecting the cavities.

For a representative specimen from Group B (Specimen Nr. 2, the standard PABST system but with a thinner primer than normal), fracture was cohesive within the adhesive, but close to the primer on the skin. This is illustrated by Figure 20 showing the fracture surface of the tee, and Figure 21 showing the fracture surface of the skin, both near the fracture initiation zone. Figure 20 shows the classical cohesive failure mode for FM73, whereas Figure 21 shows the needle-like chromate crystals from the primer under a thin layer of adhesive.

For a specimen from Group C (Specimen Nr. 2, the PABST system but with three layers of adhesive and a thinner than normal primer), the locus of fracture was predominantly cohesive within the adhesive but there were also zones of interfacial failure, namely, adhesive to primer failure, and primer to oxide failure. The interfacial failures were on the skin side. This is illustrated by Figure 22 for the tee and Figure 23 for the skin, both showing fracture surfaces near the zone of fracture initiation. Figure 22 shows the classical cohesive failure for FM73, whereas Figure 23 shows a combination of failure modes both cohesive and interfacial.

For a representative specimen from Group D (Specimen Nr. 3, FM73 adhesive on phosphoric acid anodize without a primer), failure initiated cohesively but then propagated interfacially toward the skin. Figures 24 and 25 show, respectively, the fracture surfaces of the skin and of the tee along the outer edge of the tee where the fracture initiated. The classical cohesive fracture morphology is clearly seen on both surfaces. However, as the fracture progressed,

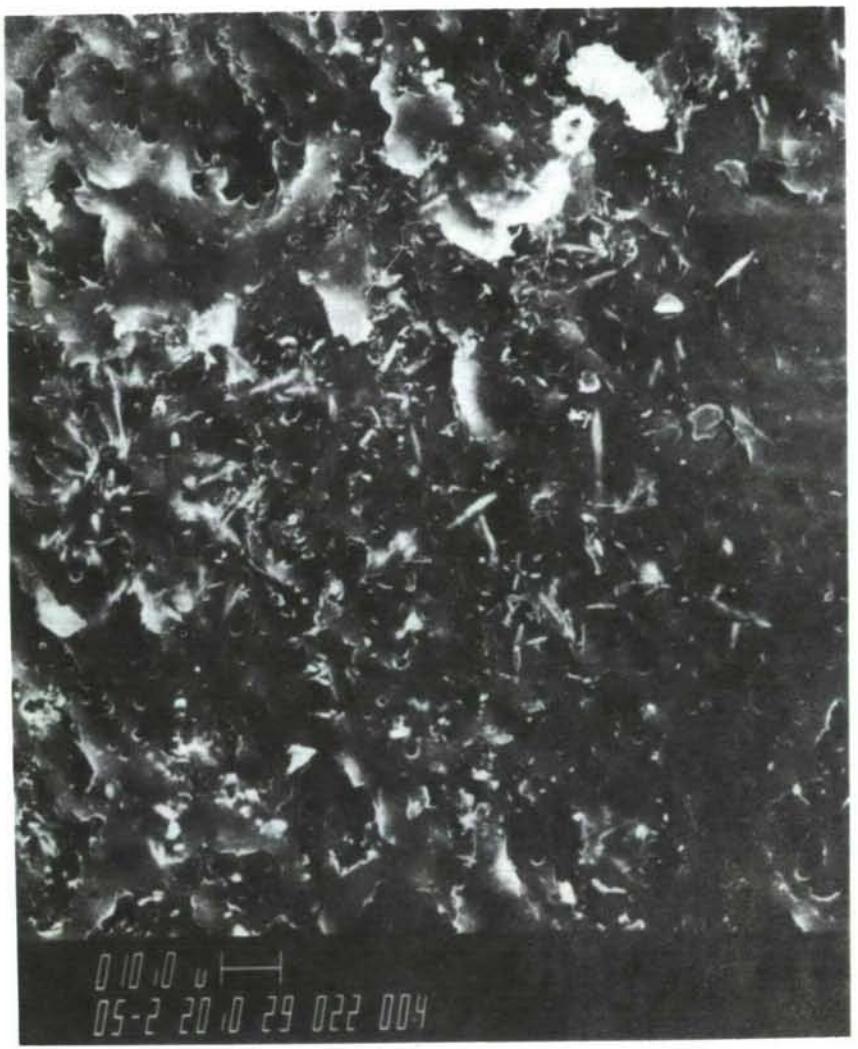

Figure Nr. 23 - Photomicrograph of Fracture Surface (Skin Side) Group C, Specimen Nr. 2

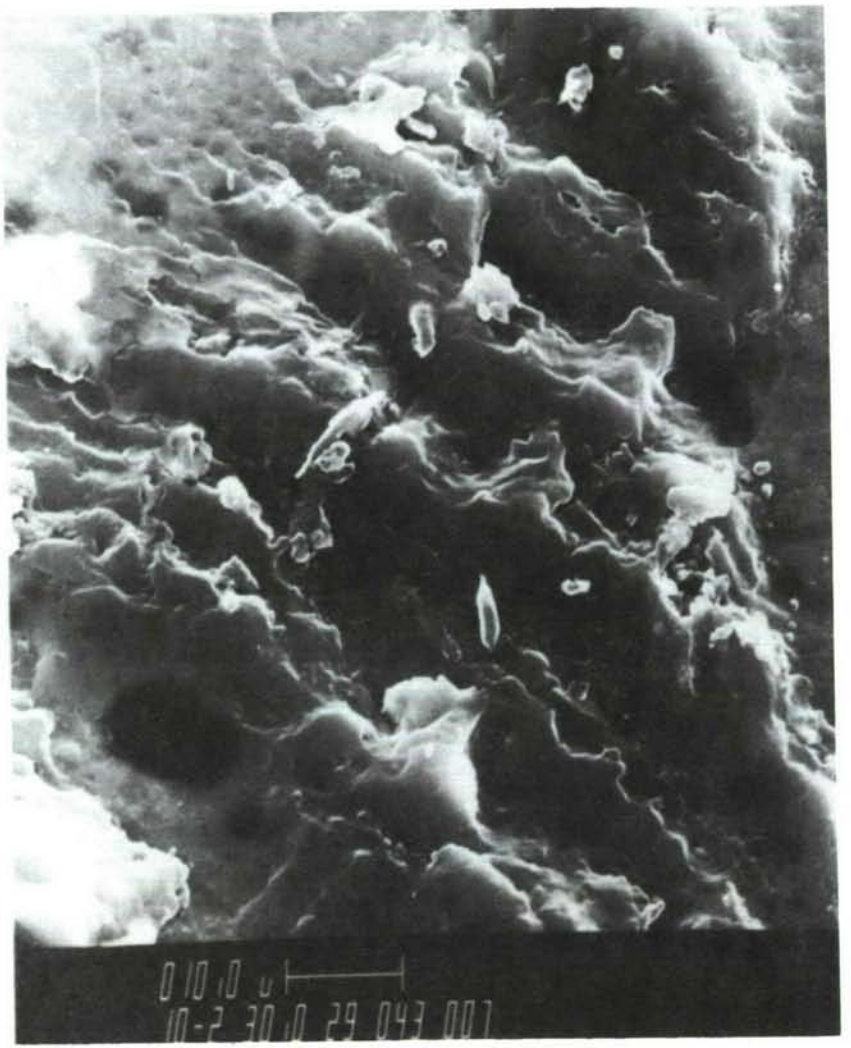

Figure Nr. 24 - Photomicrograph of Fracture Surface (Skin Side), Group D, Specimen Nr. 3

Figure Nr. 25 - Photomicrograph of Fracture Surface (Tee Side), Group D, Specimen Nr. 3

Figure Nr. 26 - Photomicrograph of Fracture Surface (Skin), Group D, Specimen Nr. 3 Near Initiation 500X

it veered toward the skin. Figure 26 shows the fracture surface of the skin about 1/8 inch (0.318 cm) from the point of initiation. This photomicrograph at 500X shows a thin layer of polymer adhering to the oxide. The pits in the adherend surface are evident, indicating that the fracture is very close to the oxide surface. One interesting feature in this photomicrograph is the presence of "lakes" of a dispersed phase in the polymer layer, rather than spherical particles. A clearer view of these "lakes" is shown at 1000X in Figure 27. The reason for the lakes is not known. However, it is speculated that they may have resulted from the high surface energy of the aluminum oxide causing sufficient spreading of the adjacent polymer layer to transform the elastomeric second phase of the adhesive into a planar, rather than a spherical configuration.

For a specimen from Group E (Specimen Nr. 3, the PABST system except using FPL etch instead of phosphoric acid anodize), the locus of fracture was purely cohesive within the adhesive, but close to the skin side. This is illustrated by Figure 28 for the tee and Figure 29 for the skin, both showing fracture surfaces near the zone of initiation. Figure 28 shows the classical cohesive failure for FM73. Figure 29 also shows cohesive failure, but along a diagonal line from upper left to lower right one can see the adherend surface through a thin layer of adhesive.

Photomicrographs of the fracture surfaces of a specimen made with AF30 (Group F, Specimen Nr. 3), a nitrile rubber phenolic adhesive, indicated predominantly cohesive fracture, but with a morphology different from that of FM73 adhesive. Figure 30 of the fracture surface of the skin shows a continuous phase which appears to be elastomeric. The elastomeric nature is indicated by local regions of "necked-down" material and the undulating, highly deformed overlapping layers. Figure 31, a photomicrograph of the

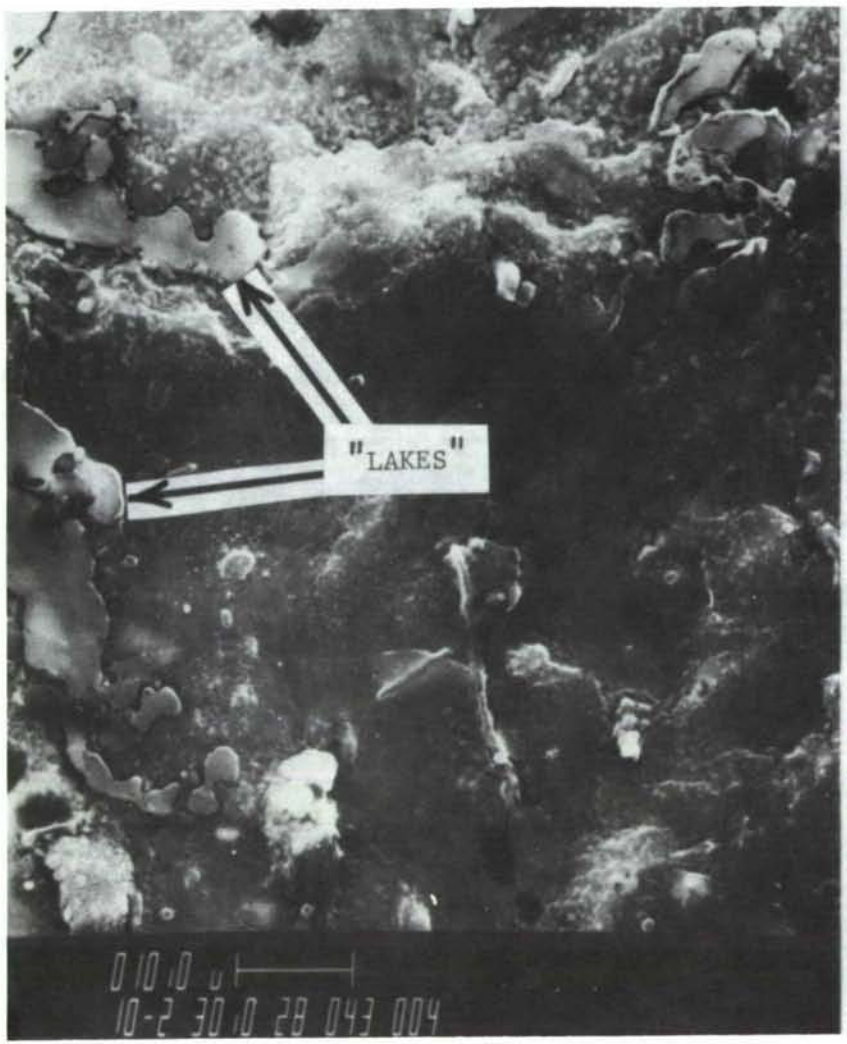

Figure Nr. 27 - Photomicrograph of Fracture Surface (Skin), Group D, Speciment Nr. 3, Near Initiation 1000X

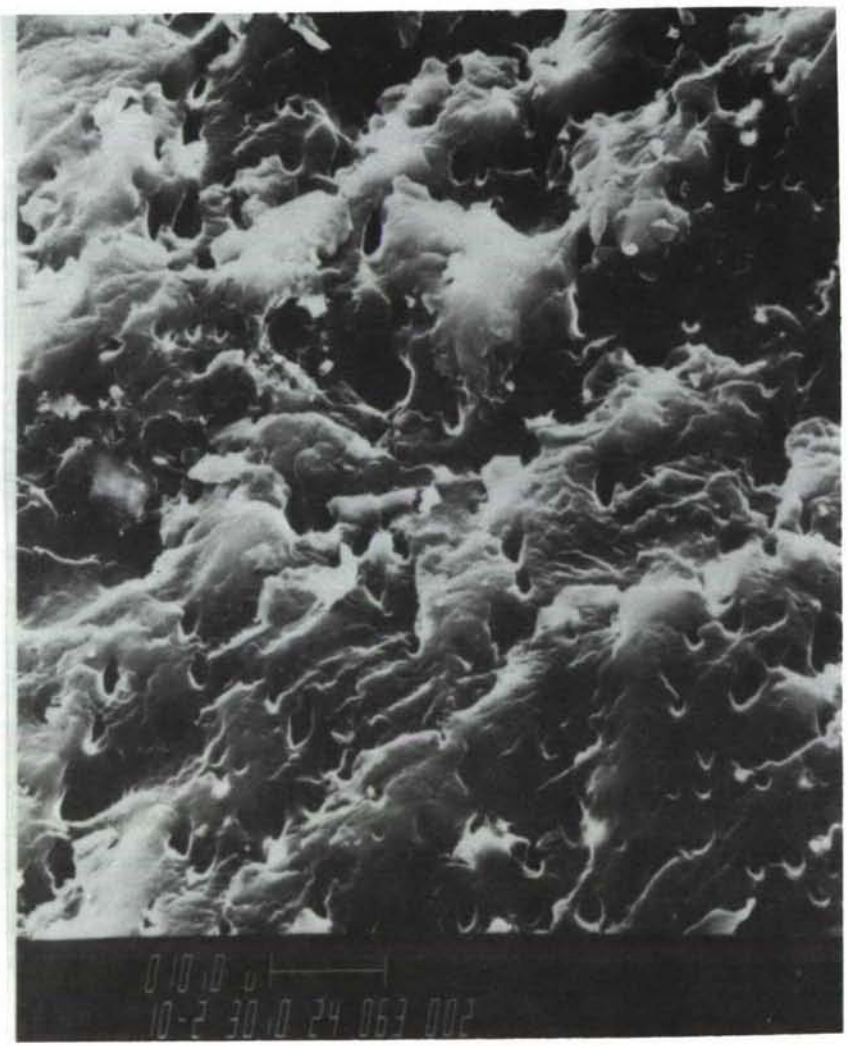

Figure Nr. 28 - Photomicrograph of Fracture Surface (Tee Side), Group E, Specimen Nr. 3

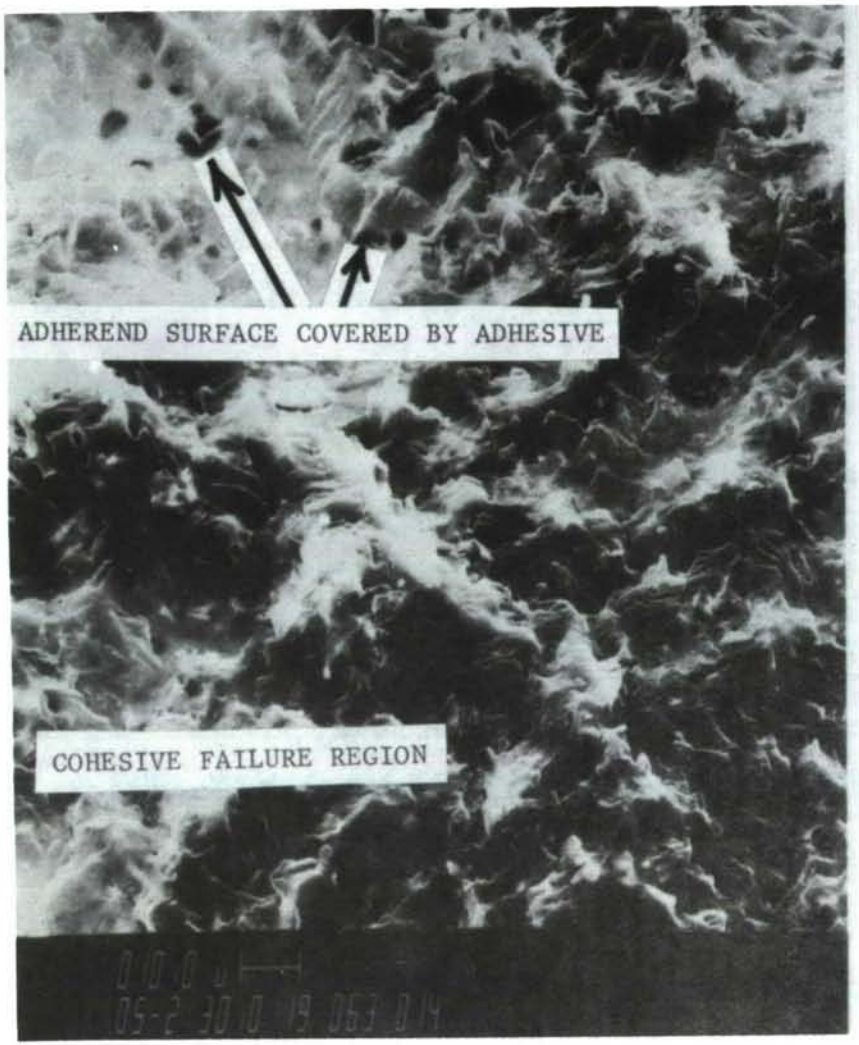

Figure Nr. 29 - Photomicrograph of Fracture Surface (Skin Side), Group E, Specimen Nr. 3

Figure Nr. 30 - Photomicrograph of Fracture Surface (Skin Side), Group F, Specimen Nr. 3

fracture surface of the tee from the same specimen, but closer to the initiation region, shows similar morphology. The presence of many loose particles may have resulted from a higher dimensional excursion during test, resulting in higher energy input and greater damage to the adhesive. Figure 32 is a photomicrograph of the flash area at the edge of the tee flange. The interesting features here are the fragmentation of the surface grains of the adherend and the separations at grain boundaries. This is presumed to have been caused by the very high energy input during the fatigue test.

The results of the fractographic investigations are summarized as follows:

a. Adhesion at interfaces (e. g. primer-to-adherend oxide and adhesive-to-primer) was generally maintained during the process of fracture propagation.

b. Fractures which visually appeared to be interfacial were usually near the primer-to-adhesive interface but in most cases had a thin layer of adhesive still bonded to the primer.

c. For the both FM73 (nitrile rubber epoxy) and AF30 (nitrile rubber phenolic) adhesives, the morphology of cohesive fractures showed that the full spectrum of fracture processes, which these adhesives are capable of undergoing, were manifested.

Figure Nr. 31 - Photomicrograph of Fracture Surface (Tee Side), Group F, Specimen Nr. 3

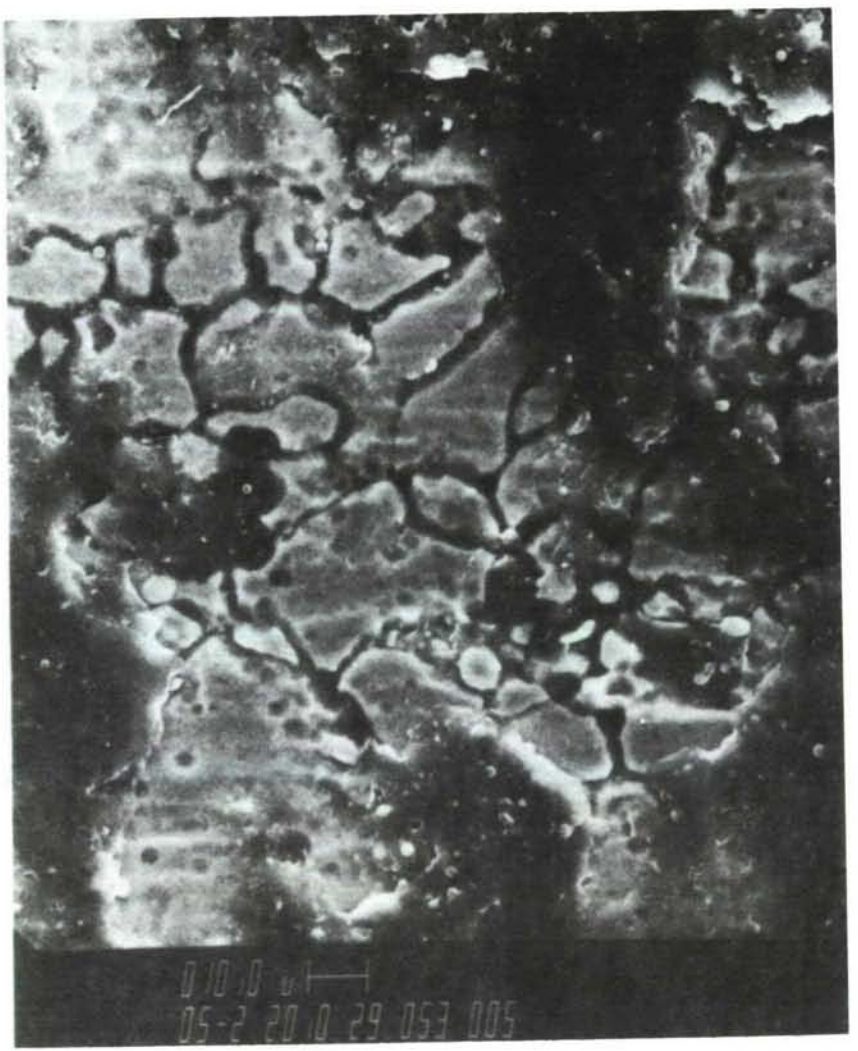

Figure Nr. 32 - Photomicrograph of Flash Area

SECTION VI

CONCLUSIONS

The double cantilever beam coupon tests provided a means of generating consistent, reproducible sonic fatigue data for adhesively bonded aluminum structures of the sheet-stringer type. The fatigue data, using the FM73/BR127 adhesive/primer system, were essentially insensitive to variations in primer thickness and type of adherend surface treatment. The beam coupons with the thicker adhesive had somewhat shorter fatigue lives and showed evidence of a failure mode that accounted for it. A slightly longer random bending fatigue life was obtained with these beam coupons than those previously tested. This was attributed to improved quality control used in the fabrication of these coupons.

The AF30 adhesive was selected in this program as having a lower modulus of elasticity and higher strain-to-fracture than FM73 adhesive. It was anticipated that, with these characteristics, it might better withstand the oscillating peel stresses due to acoustic loads. The damping data indicated that the AF30 adhesive has a significantly higher damping ratio than the FM73 adhesive. A much higher acceleration level was required to attain the desired strain level in the AF30 coupons than in the FM73 coupons. Since the AF30 coupons required more energy to reach a given strain level and have considerably higher damping properties at room temperature, it was concluded that a structure, using AF30 adhesive, would have a corresponding increase in sonic fatigue resistance at room temperature.

A failure analysis of the fractured surfaces was made using a scanning electron microscope (SEM). The failure analysis consisted of two types of observations, one being "locus-of-fracture" and the other being "fracture

mechanisms." The locus-of-fracture observations determined whether fracture was within the adhesive, at the adhesive-to-primer interface, within the primer, at the primer-to-oxide interface, or within the oxide. The fractures observed, except for Group C which had interfacial failure, were essentially all within the adhesive; however, in some cases the failures were very close to the primer surface. Fractographic observations also determined the mechanisms of fracture initiation and propagation, and noted physical features that identified energy dissipation mechanisms during fracture.

APPENDIX

PROCESS AND FABRICATION PROCEDURES USED TO PREPARE ADHESIVELY BONDED SKIN/TEE SPECIMENS

a. Adherend (7075 T-6 bare and 2024 T-3 bare aluminum alloy) surface treatments.

(1) FPL Etch ("Optimized" Version)

The adherends were vapor degreased in trichlorethylene, cleaned in a hot alkaline cleaner solution, rinsed in tap water, and then placed in FPL etch solution at 155°F (68.3°C) for 12 minutes. The FPL etch solution consisted of sodium dichromate, concentrated sulfuric acid, and distilled water in a ratio of 1:10:30 by weight. Copper was added to the solution prior to use in the form of a small piece of scrap 2024 T-3. Treated adherends were immersion rinsed in tap water followed by deionized water and then dried at 140°F (60°C).

(2) Phosphoric Acid Anodize

The procedures used followed those described in SAE's ARP 1524 and Boeing Process Specification BAC5555. They consisted of degreasing, alkaline cleaning, deoxidizing, and anodizing. The degreasing and alkaline cleaning procedures were similar to those used for the FPL etch. The deoxidizing was performed using a solution of Oakite 34 and sulfuric acid at room temperature for approximately three minutes. The anodizing was performed at room temperature using a 10% weight solution of phosphoric acid, 10 volts, and an anodizing time of twenty-two minutes.

b. Primer Application

Primers were applied by a small spray gun pressurized with bottled nitrogen gas instead of compressed air in order to avoid introducing

contaminants such as oil or water. Primer thickness was controlled by the number of "passes" with the spray gun. After spraying, the primed adherends were allowed to air dry for approximately 30 minutes. After cure, the primer thickness was measured with an eddy current type instrument. The adherends primed with BR127 were then placed in an oven at 250°F (121.1°C) for 30 minutes; those primed with EC1660 primer were placed in an oven at 225°F (107.2°C) for 30 minutes. After removal from the oven and cooling, primer thickness was measured.

c. Lay-up and Cure of Adhesive Bonded Skin/Tee Specimens

(1) Panel Lay-up

Adhesive film was placed between the flange of the tee and the skin, extending slightly beyond the edge of the tee to insure forming a fillet from the adhesive flash. Metal bars were placed on top of the tee flange so that positive pressure would be applied to the bond line during autoclave cure. The assembly was bagged in plastic and sealed. Vacuum was applied to the lay-up and it was placed in the autoclave. After applying autoclave pressure, the vacuum was vented to the atmosphere, and the heat cure cycle commenced.

(2) Autoclave Cure

(a) FM73/BR127

A pressure of 45 psi (3.10×10^5 Pascals) was applied to the FM73/BR127 panels; they were then heated from room temperature to 250°F (121.1°C) in about 30 minutes, and held there for 60 minutes.

(b) AF30/EC1660

A pressure of 100 psi (6.89×10^5 Pascals) was applied to the AF30/EC1660 panels. They were then heated from room temperature to 350°F (176.6°C) in about 40 minutes, and held there for 60 minutes.

REFERENCES

1. Rudder, F. F., Jr. and Plumbee, H. E., Jr., "Sonic Fatigue Design Guide for Military Aircraft," AFFDL-TR-74-122 (AD-B004-600L), AF Flight Dynamics Laboratory, Wright-Patterson AFB, Ohio, May 1975.

2. Belcher, P. M., Eshleman, A. L., Van Dyke, J. D., "Development of Aircraft Structure to Withstand Acoustic Loads," Aerospace Engineering Vol. 18, Nr. 6, 1959.

3. Clarkson, B. L., "Stresses in Skin Panels Subjected to Random Acoustic Loading," ISV Report, 1967.

4. Bussa, S. L., "Fatigue Life of Low Carbon Steel Under Stochastic Condition," MTS Report 900.21-1, 1967.

5. Wentz, K. R. and Wolfe, H. F., "Development of Random Fatigue Data for Adhesively Bonded and Weldbonded Structures Subjected to Dynamic Excitation," Journal of Engineering Material and Technology, Vol. 100, January 1978.

6. Rowe, E. H., Seibert, A. R. and Drake, R. S., "Toughening Thermosets with Liquid Butadiene/Acrylonitrile Polymers," Modern Plastics, August 1970.

7. Rowe, E. H. and Riew, C. K., "What Failure Mechanisms Tell About Toughened Epoxy Resins," Plastics Engineering, March 1975.

8. Drake, R. and Seibert, A., "Elastomer-Modified Epoxy Resins for Structural Applications," SAMPE Quarterly, Vol. 6, Nr. 4, July 1975.

☆U.S.Government Printing Office: 1981 — 559-005/4005